Chapter 1

Introduction

1.1 Historical background

"The optimists say solar power could become as economical and efficient as fossil fuels. The pessimists say they've heard all this before" (Johnson, 2009).

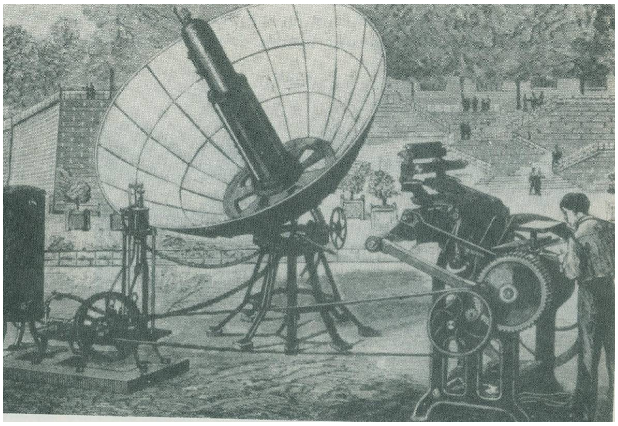

Figure 1.1 A parabolic collector powering a printing press at the 1878 Paris Exposition (Kreith and Kreider, 1978).

The interest and research in solar power have come a long way. Cheremisinoff and Regino (1978) acknowledge the history of solar energy and solar energy availability from the years before Christ up to the 1970s. According to Kreith and Kreider (1978), a diamond was melted for the first time in 1695 in Florence by an early solar practitioner. They also mention that solar combustion experiments were done by the French chemist, Lavoisier, and the English scientist, Joseph Priestley, in 1774. In 1878, a solar steam engine, using a parabolic reflector reflected onto a steam boiler, was exhibited at the World Fair in Paris. This engine, shown in Figure 1.1, was utilised to run a printing press.

In 1901, a 7.5 kW solar steam engine was operated by AG Eneas in Pasadena, California. The focusing collector is shown in Figure 1.2. Between 1907 and 1913, the American engineer F Shuman, developed solar-driven hydraulic pumps. There was very little activity in the field of solar power between 1915 and 1950. The interest was revived in 1949 and in the 1960s, as the objective of NASA's research and development programme was to build a solar electric power

system capable of supplying electricity for the US space programme. Research funds became available and widespread interest grew for the development of earth-bound solar electric power, which increased after the oil crisis in 1973 (Kreith and Kreider, 1978).

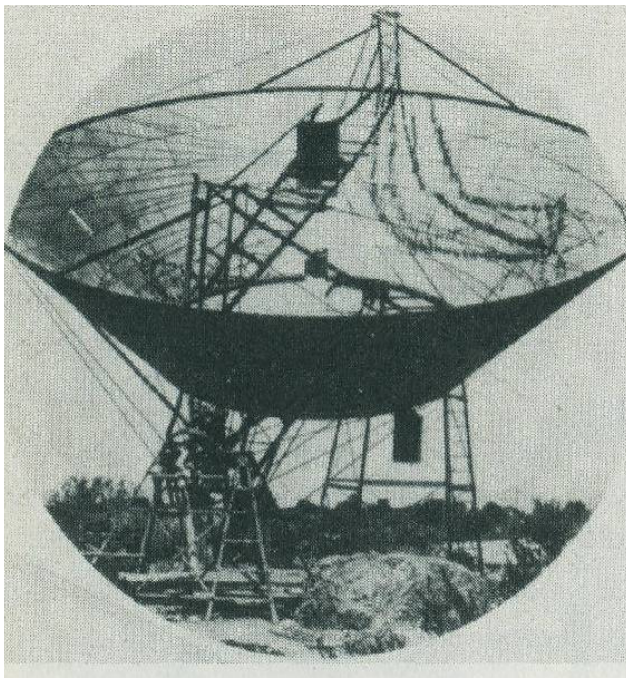

Figure 1.2 A solar-powered steam engine in Arizona in the early 1900s (Kreith and Kreider, 1978).

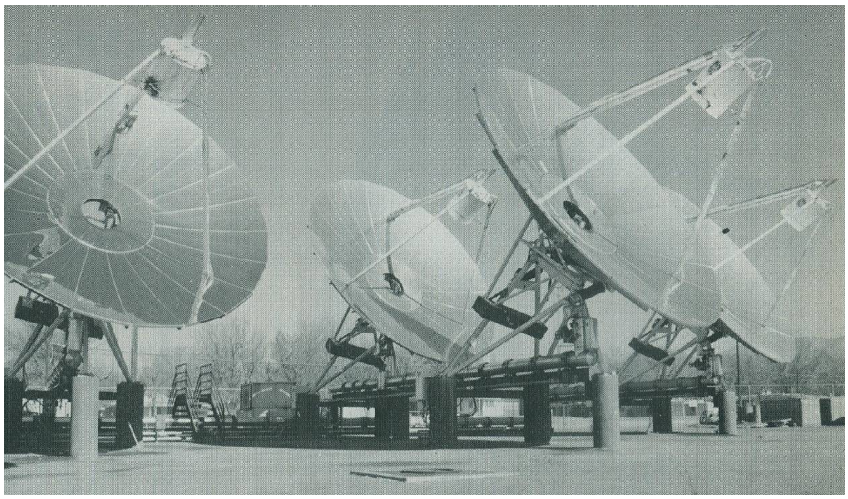

Figure 1.3 Commercially produced point focus concentrators (Howell et al., 1982).

Figure 1.3 shows the Shenandoah solar total energy project at Shenandoah, Georgia, which was installed before 1983. It was designed for application to a solar thermal co-generation project and was commercially procured (Howell et al. 1982; Stine and Harrigan, 1985). The national crisis in 1973 and soaring oil prices in 1979, created a great sense of urgency and called for research into

renewable energy in the US. In 1977, President Jimmy Carter called for a federal push for renewable energy. Nine large solar thermal plants were installed before oil prices plummeted and President Carter left office, leaving solar energy as a minor factor in the energy equation (Johnson, 2009).

Today is a new dawn for solar power. A call for clean and efficient energy can be heard all over the world to ensure a safe and stable environment.

1.2 Problem

South Africa, like southern Africa, has much potential to generate large amounts of its power from solar technologies. Kreith and Kreider (1978) state that there are technological and natural types of solar radiation collections. Natural collection includes phenomena such as wind and ocean temperature differences. There are two main research fields concerning the harnessing of the sun's power: concentrated solar power (or solar thermal power) and photovoltaic panels, which are respectively ±24% and 10-20% efficient in converting the sun's energy into electricity (Johnson, 2009). Concentrated solar power systems use the concentrated power of the sun as a heat source to generate mechanical power.

Fluri (2009) shows that the total potential generation capacity of large-scale concentrated solar power in South Africa is more than 500 GW, when using the best suitable locations for large-scale power plants in the country. These locations, as identified by Fluri (2009), are areas which have sufficient sunshine, are close enough to transmission lines, are flat enough, where the respective vegetation is not under threat and which have suitable land-use profiles. According to Fluri (2009), the solar irradiation in the northern parts of the Northern Cape Province, South Africa, is more than 8 kWh/m^2 in December and 6 kWh/m^2 in June. Most areas in South Africa, however, receive an average of more than 2 500 hours of sunshine per year, with average solar-radiation levels ranging between 4.5 and 6.5 kWh/m^2 per day (DME, 2010), which makes small-scale concentrated solar power applications equally attractive.

Thus far, the world's solar leaders are not necessarily the sunniest countries, but rather the ones that can afford to pay extra for solar power (Johnson, 2009). It is therefore very important to understand the costs involved in solar power and to be able to get the best efficiency from these solar power systems.

Different types of solar thermal power systems exist. According to Chen et al. (2007), the Brayton cycle is definitely worth studying when comparing its efficiency with those of other power cycles. Mills (2004) argues that emphasis may shortly shift to solarised Brayton micro-turbines from Dish-

Stirling technology due to high Stirling engine costs. The highest-efficiency Brayton cycles are regenerative cycles with low pressure ratios (Stine and Harrigan, 1985). The fact that the Brayton cycle can be an open cycle (which means air can be used as working fluid), makes this cycle very attractive for use in the water-scarce southern Africa. The small-scale open and direct solar thermal Brayton cycle with recuperator has several advantages, including lower cost, low operation and maintenance costs and it is highly recommended. The main disadvantages of this cycle are the pressure losses in the recuperator and receiver, turbomachine efficiencies and recuperator effectiveness (Stine and Harrigan, 1985), which limit the net power output of such a system. Maximum net power output is required for a small-scale solar thermal Brayton cycle with recuperator. The net power output can for example be used to drive an electrical generator and the higher the net power output the more electricity can be produced. To obtain this maximum net power output, a combined effort of heat transfer, fluid mechanics and thermodynamic thought is required. Bejan (1982) suggests that the method of entropy generation minimisation combines these thoughts.

The irreversibilities of the recuperative solar thermal Brayton cycle are mainly due to heat transfer across a finite temperature difference and fluid friction. Various studies have emphasised the importance of the optimisation of the global performance of a system, by minimising the sum of the irreversibilities from all the different components or processes of the system (spreading the entropy generation rate through the system by optimally sizing the hardware, in stead of optimising components individually). This emphasis is made by Bejan (1996; 1997), Bejan et al. (1996), Ordóñez and Bejan (2000), Shiba and Bejan (2001) and Zimparov et al. (2006a; 2006c). For the open and direct solar thermal Brayton cycle, an optimisation of this kind is not available from the literature. The geometries of the receiver and recuperator can be optimised in such a way that the total entropy generation rate is minimised to allow maximum net power output.

1.3 Purpose of the study

The objective of this study is to apply the second law of thermodynamics and entropy generation minimisation to optimise the components in a solar thermal power system such that the system produces maximum net power output at steady-state. An analysis is done by looking at the solar thermal power system as a whole and by minimising the total entropy generation rate in the system, instead of optimising components individually. In a solar thermal Brayton cycle with a micro-turbine operating at its highest compressor efficiency, geometric variables of a modified cavity receiver, proposed by Reddy and Sendhil Kumar (2009), and a plate-type counterflow recuperator (Shah, 2005) are optimised. The surface temperature of the receiver should stay below 1 200 K due to material constraints. The dynamic trajectory optimisation method for constrained optimisation (Snyman, 2000) is used. Off-the-shelf micro-turbines (Garrett, 2009)

chosen for low cost, high availability and reliability and a range of parabolic dish concentrator diameters are considered. The technical data of these micro-turbines are also available. A valuable understanding of the optimal distribution of the total entropy generation rate (or irreversibility rate) throughout the open and direct recuperative solar thermal Brayton cycle should be obtained. The effect of various environmental conditions and constraints on the optimum geometries is investigated.

In this study, the open and direct solar thermal Brayton cycle with recuperation is analysed at different steady-state conditions and parameters. The geometries of a modified cavity receiver and counterflow plate-type recuperator are optimised so that the system produces maximum net power output. The net power output of the system is described in terms of the total entropy generation rate within the system. The net power output of the system is maximised, the total entropy generation rate is minimised and the geometries of the receiver and recuperator are optimised.

1.4 Layout of dissertation

At the outset, a literature survey is conducted in Chapter 2. Solar thermal power systems are investigated and compared. Solar collectors and recuperators are explored as well as the second law of thermodynamics and its application to these components. From the literature survey, the problem is formulated in Chapter 3 and the model is described in Chapter 4. An objective function is constructed and the numerical optimisation method is given. In Chapter 5, the results and a validation are presented. Optimum geometries and operating conditions are given for different environmental conditions. The possibilities for future work are examined and in Chapter 6, the concluding remarks are made.

Chapter 2

Literature survey

2.1 Introduction

In this chapter, a literature survey is conducted. Different solar thermal power systems are considered and compared. The solar thermal Brayton cycle is chosen for further investigation. Solar collectors and recuperators are explored as well as the second law of thermodynamics and its application to these components. An overview of concepts such as the second law of thermodynamics, exergy and entropy is given. Entropy generation and its minimisation are introduced and its application to the solar thermal Brayton cycle is identified. Solar radiation and the exergy of solar radiation are explored. Lastly, the concluding remarks are made.

2.2 Solar thermal power systems

2.2.1 Background

Duffie and Beckman (1991) describe solar thermal power systems as the conversion of solar to mechanical and electrical energy. Much of the early solar thermal power systems were for small-scale applications of up to 100 kW (mostly used for water pumping), while after 1975 many large-scale power systems were built in the megawatt range. Three power cycles are mainly considered for solar applications or solar thermal power systems: the Rankine, Stirling and Brayton cycles (Bejan, 1997; Stine and Harrigan, 1985). Brayton and Stirling engines provide high engine efficiencies, but are limited by low gas heat transfer coefficients, which would require large receivers and cavity receivers. The Rankine cycle allows for smaller receivers, which can use fluids with high heat transfer coefficients (Duffie and Beckman, 1991). According to Mills (2004), the Rankine cycle appears to be the best option with trough plants because of temperature limitations in the latter, and Brayton cycle micro-turbines appear to be moving quickly to displace Stirling engines in the two-axis tracking market because of much lower cost. The efficiency of a solar thermal receiver diminishes as its operating temperature rises, while the efficiency of the cycle rises as the operating temperature rises (Duffie and Beckman, 1991; Stine and Harrigan, 1985). It is clear that an optimum operating temperature must exist. For example, Stine and Harrigan (1985) give an operating temperature of 780°C as the optimum for a concentrator when combined with a Carnot-engine.

2.2.2 Power cycles available for solar thermal application

2.2.2.1 The Rankine cycle

According to Stine and Harrigan (1985), the most common cycle used in solar power systems is the Rankine cycle with water, organic liquids or liquid metals as the working fluid. The Rankine cycle is shown in Figure 2.1. Reheating and regeneration can also be used. Stine and Harrigan (1985) also claim that most solar power cycles in operation or under development are Rankine cycles.

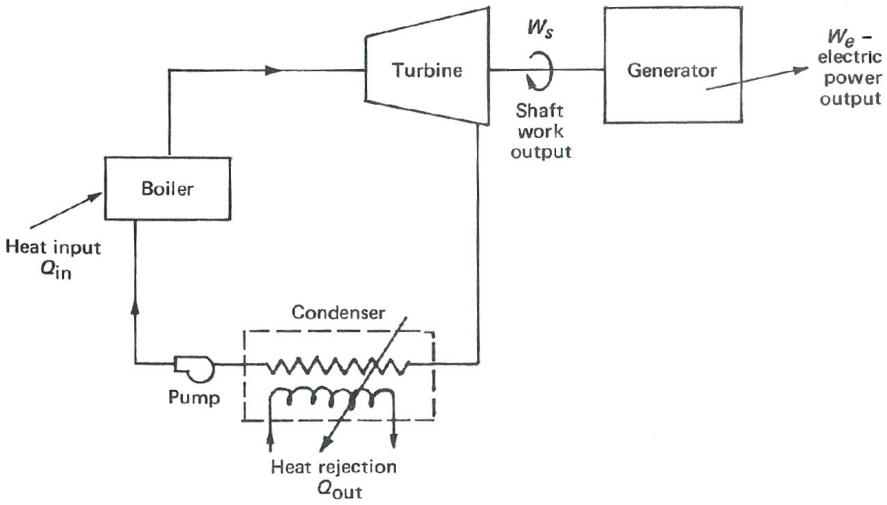

Figure 2.1 The Rankine cycle (Kreith and Kreider, 1978).

The most common condenser for the Rankine cycle is considered to be a shell-and-tube heat exchanger, requiring a supply of cooling water. The radial-flow and axial-flow turbines are considered to be the most common turbines used with the Rankine cycle. The radial-flow turbine is considered to be more efficient for small power output applications (Stine and Harrigan, 1985). An interesting example of a solar Rankine cycle delivering between 10 – 100 kW is a cycle designed for the US Department of Energy's Small Communities Project by Barber-Nichols Engineering (Stine and Harrigan, 1985). It is designed to produce 26 kW of shaft power with a peak operating temperature of 400 ℃, with toluene as working fluid. The turbine rotates at 60 000 rpm and has a mean blade diameter of 12.5 cm. The engine has a thermal efficiency of 24%. STG International (2010) uses an organic Rankine cycle for its solar concentrator module. The module produces 3 kW of electrical power with parabolic trough concentrators.

2.2.2.2 Stirling engines

According to Stine and Harrigan (1985), the Stirling engine placed at the focus of a parabolic dish concentrator is being proposed for many small (10 – 100 kW) solar power applications because

of its high cycle efficiency potential (a Stirling engine can be designed to have the same efficiency as the ideal Carnot cycle). Three major causes of inefficiencies in the Stirling engine exist: sinusoidal motion of the pistons, imperfect regeneration and dead volume (Stine and Harrigan, 1985). Figures 2.2 and 2.3 respectively show an example of a Stirling engine and the T-s diagram of the ideal Stirling cycle.

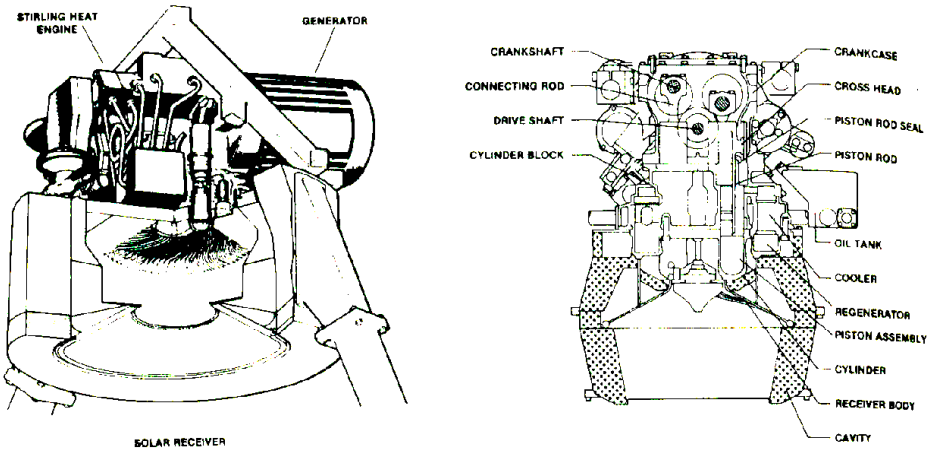

Figure 2.2 The United Stirling Model 4-95 solar Stirling engine (Stine and Harrigan, 1985).

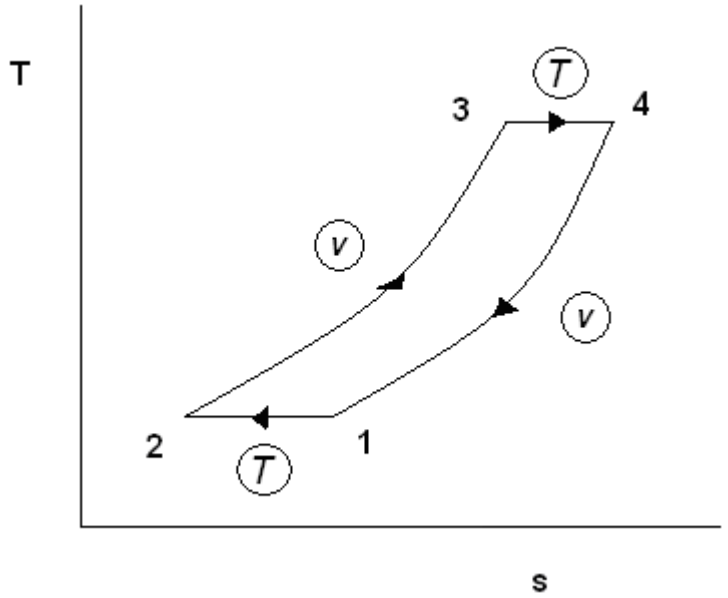

Figure 2.3 The four processes of an ideal Stirling engine cycle.

An example of a Stirling engine is the Solar 4-95 engine, which produces 22 kW of shaft power at a thermal efficiency of 38%. The heater operates at 720℃ (Stine and Harrigan, 1985). One should take note of the free-piston Stirling engine (Stine and Harrigan, 1985). This engine was developed in an attempt to get around the problem of sealing the engines from gas leakage and

to eliminate mechanical friction associated with bearings, crossheads and seals. In this design, a power piston and a displacer bounce back and forth in a harmonic motion with mechanical or gas springs causing reversal of the motion. The engine has a diameter of 3.35 cm and a stroke of 2 cm and produces 100 W of alternating current electrical power with a frequency of 30 Hz when heated to 650℃.

2.2.2.3 The Brayton cycle

Chen et al. (2007) show that the Brayton cycle is definitely worth studying when comparing its efficiency with that of other power cycles. Mills (2004) predicts that emphasis may shortly shift from Dish-Stirling technology to solarised Brayton micro-turbines due to high Stirling engine costs. The lower Brayton costs are due to high production quantities in the current market. Mills (2004) argues that the efficiency of the Brayton cycle is 25 - 33%, while the efficiency of the Stirling engine is 42%. However, according to Mills (2004), it is possible for Brayton cycles to reach peak efficiencies close to 40%.

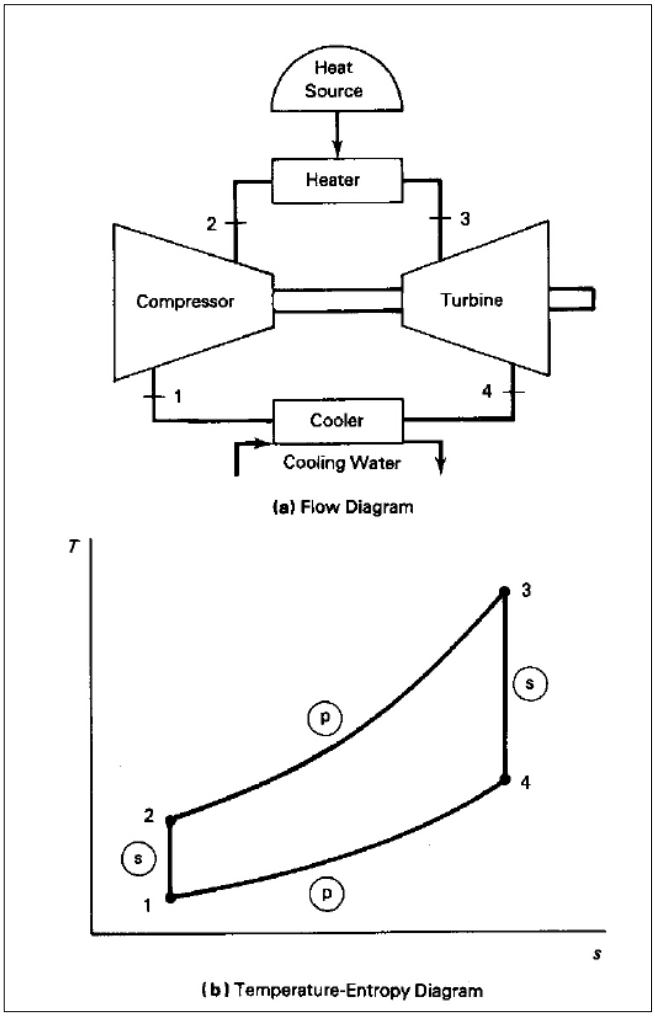

Figure 2.4 The Brayton cycle (Weston, 2000).

A flow diagram of the Brayton cycle, showing the requirement of a heat source, is given in Figure 2.4. This heat source is usually provided by fuel combustion. However, it can also be provided by solar energy. The Brayton cycle is considered for both small-scale and large-scale power applications, with its potential for low operation and maintenance cost as its major advantage. These engines are proposed to be placed at the focus of a parabolic dish concentrator. Operating at relatively low pressure, the Brayton cycle requires large, hot gas receivers. Its major drawback is the high receiver operating temperatures required to get reasonable efficiencies. Most Brayton cycles are not self-sustaining at operating temperatures below 480℃ (Stine and Harrigan, 1985).

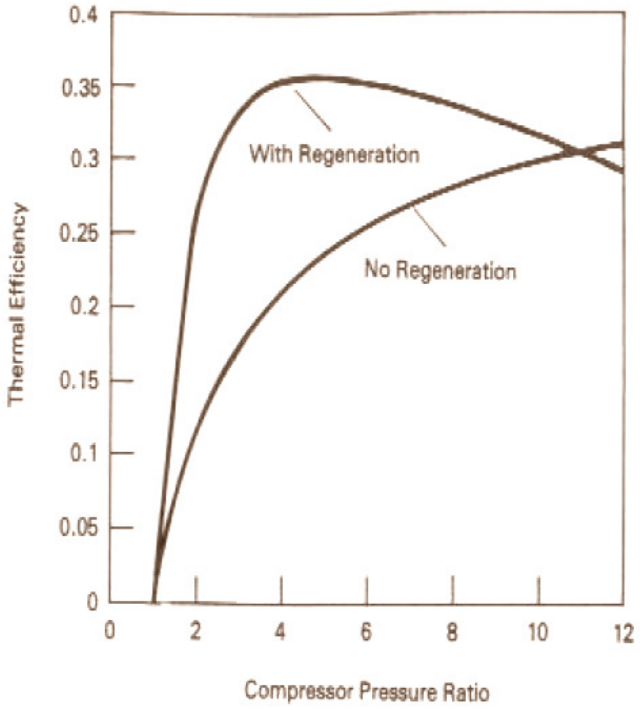

Figure 2.5 The thermal efficiency of a two-shaft gas turbine cycle with and without regeneration, as plotted from an example spreadsheet for different pressure ratios (with recuperator efficiency < 1) (Weston, 2000).

A recuperator (heat exchanger) can be used in the Brayton cycle to extract the heat from the turbine outlet and transfer it to the cold stream before it is heated by the heat source. The effect of regeneration on the thermal efficiency of a Brayton cycle is shown in Figure 2.5. From Figure 2.6, it is concluded that the highest-efficiency Brayton cycles are regenerative cycles with low compressor pressure ratios. If regeneration is not used, high compressor pressure ratios are required to provide high efficiency.

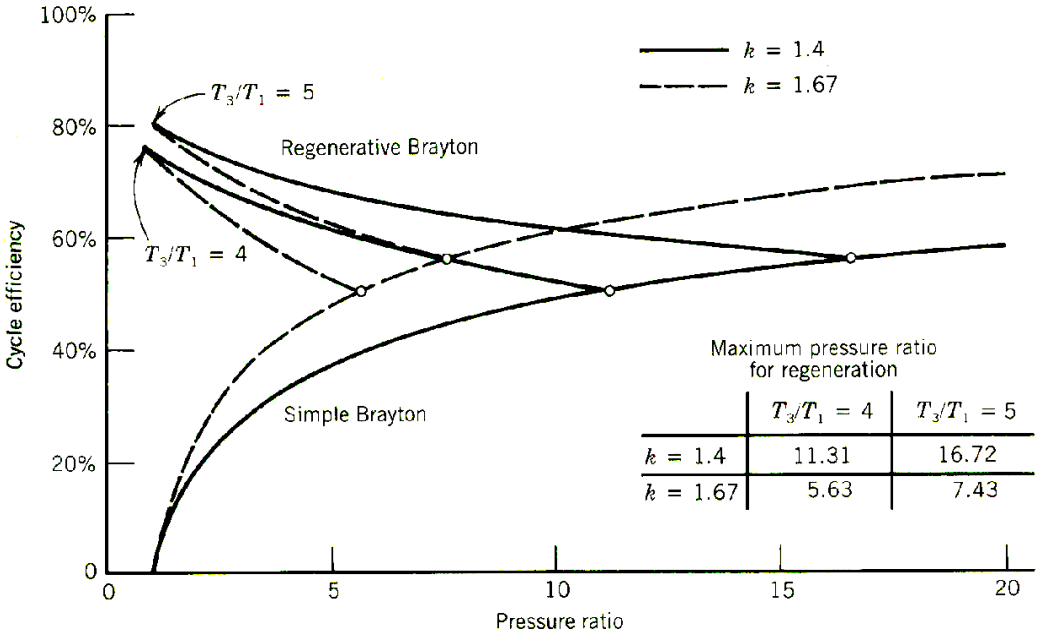

Figure 2.6 The regenerative Brayton cycle efficiency compared with the simple cycle efficiency. These curves are for a recuperator efficiency of 100% (Stine and Harrigan, 1985). Temperature values correspond to the values in Figure 2.4b and $k = c_p / c_v$.

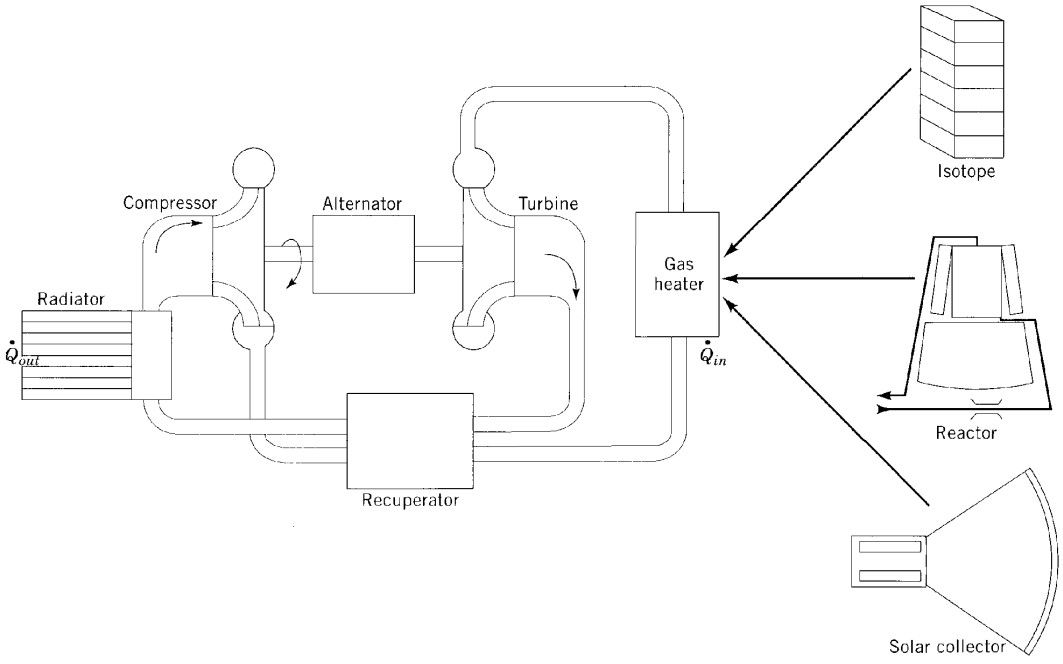

Figure 2.7 A closed Brayton cycle power plant for use in space (Bejan et al., 1996).

An extra heat exchanger can be used to extract heat from the fluid system in direct contact with solar radiation (making the system an indirect system). A radiator might also be used in a closed Brayton cycle. Figure 2.7 gives an example of a closed Brayton cycle for use in space. Bejan et al. (1996) imply that the solar heat source is more suitable than the isotope and nuclear heat

sources when the power plant size is in the range of 2 – 100 kW. Helium has been proposed for closed solar Brayton cycles because of its efficiency advantage plus its high heat transfer capability and because it is inert. For open Brayton cycles, it is essential to have natural air movement past the site to prohibit reinjection of the warm exhaust (Stine and Harrigan, 1985).

Heat exchangers can also be used for intercooling and reheating in a solar thermal Brayton cycle. The major advantage of multistaging (combining a number of compression and expansion stages in series with coolers and heaters respectively) is that the cycle can have the high efficiency associated with low-pressure ratio regenerative cycles, without the extremely large recuperator required for a single-stage cycle of the same power output (Stine and Harrigan, 1985). Maximum efficiency is attained when equal pressure ratios are maintained across each compressor and each turbine stage. The Ericsson cycle has the potential of attaining Carnot efficiency when regeneration is used (Stine and Harrigan, 1985).

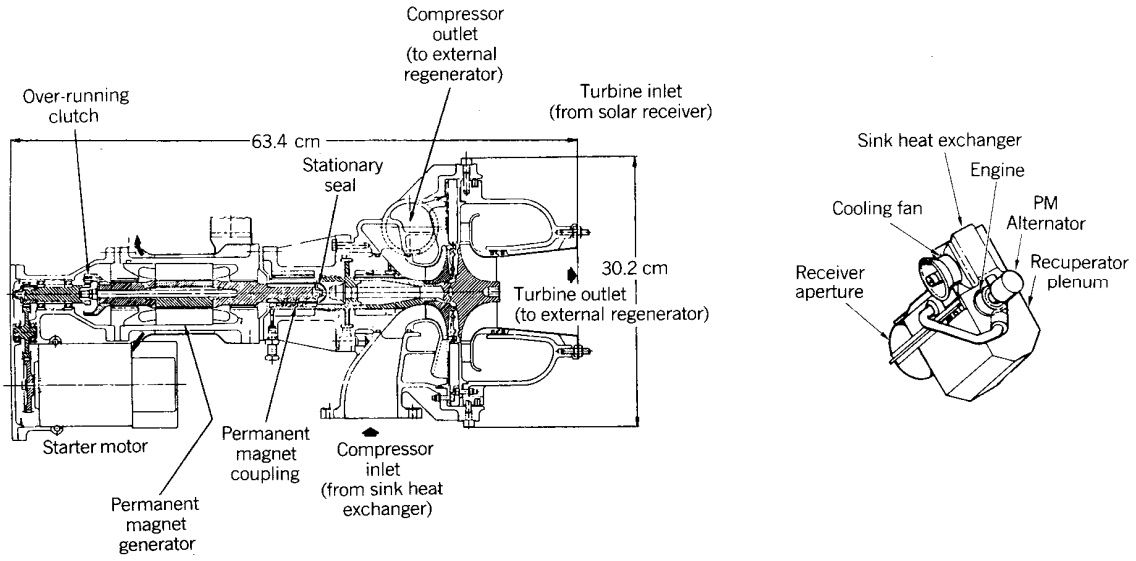

Figure 2.8 A solar sub-atmospheric gas turbine engine for parabolic dish application (Stine and Harrigan, 1985).

According to Stine and Harrigan (1985), there are three major losses in actual Brayton cycle engines: duct pressure losses, turbomachine efficiencies and recuperator effectiveness. Figure 2.8 shows the sub-atmospheric Brayton cycle, an example of the closed Brayton cycle where heat is added to the receiver at atmospheric pressure and rejected at a lower pressure. The receiver design is greatly simplified, which allows for large blade heights in the turbine and compressor. This results in higher efficiencies. According to Stine and Harrigan (1985), such a system's shaft would operate at 71 000 rpm, while air is heated to 871°C and 11 kW of electric power is produced at a cycle efficiency of 27%. The SAGT (a solar version of the Garrett Turbine Engine Company's automotive gas turbine engine), shown in Figure 2.9, is another example. It is

an open cycle with regeneration provided by a rotary porous ceramic wheel regenerator. It operates at 87 000 rpm, a peak pressure and temperature of 0.5 MPa and 1371℃ and at a cycle efficiency of 47% while it produces 75 kW of power (Stine and Harrigan, 1985).

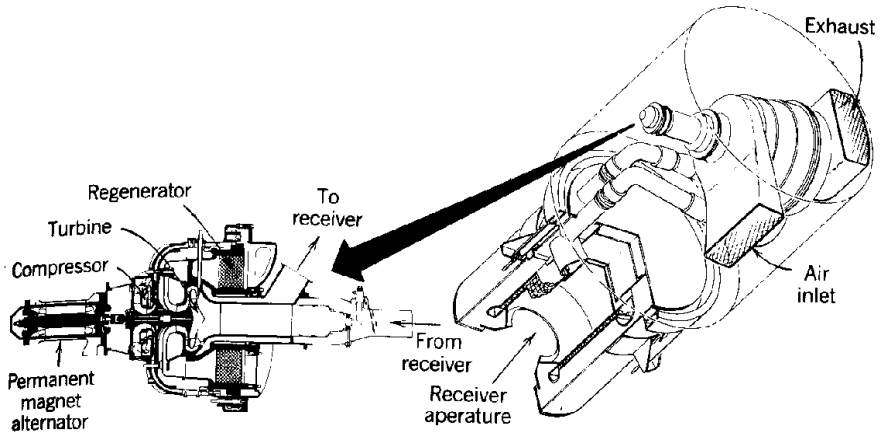

Figure 2.9 A solar version of the Garrett Turbine Company's Brayton cycle automotive gas turbine engine (Stine and Harrigan, 1985).

2.2.2.3.1 Compressors, turbines and the Brayton cycle: micro-turbines

Tsai (2004) explains the design and performance of a gas turbine engine using an automobile turbocharger. The net power output available from this specific system is close to 22 kW. Honeywell Garrett micro-turbines are widely available in South Africa, thanks to the motor industry. Shah (2005) regards the Honeywell turbomachinery as worth mentioning when it comes to the company's development expertise in micro-turbines in recent history. The Garrett range is very attractive from a cost, availability and reliability perspective. Very useful data are also made available at no cost. For each of its micro-turbines, data are available, including compressor and turbine maps. This could not be found as convincingly from other leading micro-turbine manufacturers. These compressor maps show that for each pressure ratio of the compressor, a specific mass flow rate exists for a specific compressor efficiency. Figure 2.10 shows a micro-turbine from the Garrett range.

It is important to know what the maximum operating temperatures of the turbines in the Garrett range are. According to Tsai (2004) and Shah (2005), a maximum operating temperature exists for micro-turbines. According to Garrett (2009) and Shah (2005), it seems that this maximum is more or less 950℃ for the inlet temperature of the turbine and 1050℃ intermittently. The air leaving the solar receiver is thus restricted to this maximum temperature. Thus, the solar receiver's surface temperature would have to be higher than 950℃ to produce these air temperatures at the turbine.

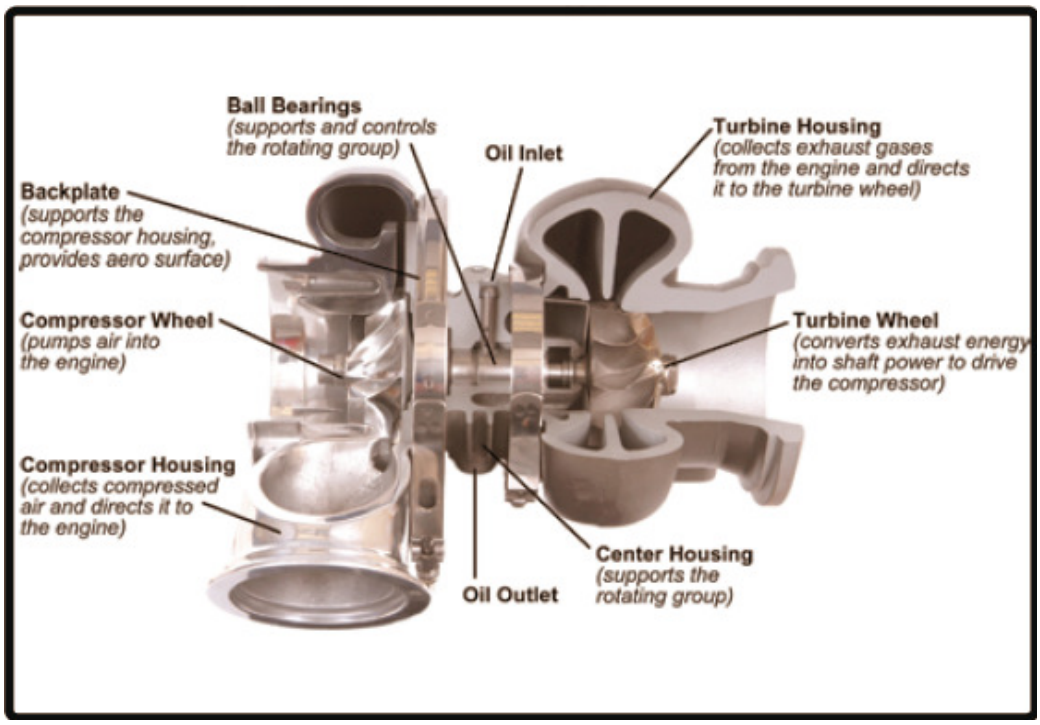

Figure 2.10 A section view of a micro-turbine from the Garrett range (Garrett, 2009).

2.2.2.3.2 Storage for the Brayton cycle

Some disadvantages of the solar thermal Brayton cycle using air as working fluid are that it has few storage options and the receiver and recuperator have to be large. This section shows possibilities for storage in the Brayton cycle, for interest's sake. Bejan (1997) suggests the use of two different working fluids and a melting element for storage. The one fluid transports the heat from the collector to the melting element while the other would be the working fluid in the Brayton cycle, which uses the temperature of the melting element as its heat source. This is called an indirect Brayton cycle and is useful when storage is necessary. An air-rock thermal energy storage system, presented by Stine and Harrigan (1985), is another heat storage option that would be compatible with a Brayton cycle. Magnesium oxide bricks are used together with a hot gas (air or helium) to store heat when extra energy is available, and to extract heat when the solar energy input is low.

2.2.3 Comparison of solar thermal power cycles

In this section, the different solar thermal power cycles are compared. It is important to keep in mind that these cycles are compared for use in South Africa in the range of 2 – 100 kW. Table 2.1 shows the advantages and disadvantages, summarised from the aforementioned text, for the Rankine, Stirling and Brayton solar thermal power cycles.

Table 2.1 Solar thermal power cycles compared (Stine and Harrigan, 1985).

	Advantages	Disadvantages
Rankine	• High heat transfer coefficients - smaller receivers • Most common and most systems in operation or under development • Low operating temperature	• Condenser required (shell-and-tube most common)
Stirling	• High efficiency (can approach ideal Carnot) • Proposed for small applications • Free-piston Stirling engine	• Low gas heat transfer coefficients - large receivers • Inefficiencies: Sinusoidal motion of the pistons, imperfect regeneration, dead volume and not all the gas in the engine participates in the cycle • Seal the engines from gas leakage and eliminate mechanical friction associated with bearings, crossheads and seals
Brayton	• High efficiency, Ericsson cycle – multistaging • Use of recuperator allows highest thermal efficiency at low pressure ratios • Both large- and small-scale application • Low operation cost, low maintenance cost • Open cycle, air – cheap • Solar heat source is more suitable than the isotope and nuclear heat sources when the power plant size is in the range of 2 – 100 kW	• Low gas heat transfer coefficients - large hot gas receivers required • Most Brayton engines are not self-sustaining at operating temperatures below 480°C • Large recuperators required • Major losses in actual Brayton cycle engines: duct pressure losses, turbomachine efficiencies and recuperator effectiveness

The Brayton cycle (Figure 2.4) looks very attractive since its low operation and maintenance costs are valuable. It can also be noted that recuperation in the Brayton cycle not only increases the thermal efficiency, but also allows for lower pressure ratios, which is very beneficial from a design perspective. The fact that the Brayton cycle can be an open cycle and that it uses air, which can be modelled as an ideal gas, makes this cycle very attractive for use in the water-

scarce southern Africa. The Brayton cycle definitely has its disadvantages as well. One of the most important disadvantages is that it is not sustainable at temperatures below 480℃ (Stine and Harrigan, 1985). According to Duffie and Beckman (1991), the energy lost from ducts and pipes leading to and returning from the solar receiver can be significant. Other important disadvantages are the pressure losses in the ducts, recuperator and receiver, turbomachine efficiencies and recuperator effectiveness. The method of entropy generation minimisation can be used to tackle these disadvantages to optimise the receiver and recuperator and to maximise the net power output of the system.

2.2.4 Comparison of working fluids and intermediate fluids

Heat transfer fluids used in central receivers, which are used on centrally located towers, are compared with the information given by Stine and Harrigan (1985) in Table 2.2.

Table 2.2 Comparison of fluids used in solar thermal power cycles (Stine and Harrigan, 1985).

	Max. temp. (℃)	Cost	Freeze (℃)	Positive	Negative
Heat transfer oils	425	High	-10	Low vapour pressure – thermal storage	Flammable
Steam	540	Low	0		De-ionised water
Nitrate-salt mixtures	565	Medium low	140 - 220	Good for storage	
Liquid sodium	600	Very high	98	Storage, low vapour pressure	
Air or helium	850	Free or very low	N.A.	Free	Few and difficult storage methods, large diameter piping required

A question might come to mind: would the efficiency of the overall system be more when the heat-extracting fluid in the receiver is also the working fluid (a direct system)? Would this efficiency be higher than when a specifically chosen optimal fluid extracts heat from the receiver, separately from an optimally chosen working fluid in the power cycle (where heat is exchanged from one to another in the heat exchanger)? It might be better to have the same fluid to perform both functions at once, while at the same time less irreversibilities are generated. According to Duffie and Beckman (1991), there is a penalty involved when such a heat exchanger is included in the system (indirect system). The system would require a larger collector concentrator to

operate at the same temperature as it would have done without the heat exchanger. Stine and Harrigan (1985) and Duffie and Beckman (1991) compared the abovementioned sides of the argument. The advantages and disadvantages of having a direct or indirect cycle/working fluid are given in Table 2.3.

Table 2.3 Advantages and disadvantages of having a direct or indirect cycle/working fluid (Stine and Harrigan, 1985).

	Direct working fluid	Intermediate fluid
Advantages	➢ Concept is simple ➢ Engine can operate at higher temperature ➢ Fewer components and no extra heat loss	➢ Reduces size and weight of receiver ➢ Reduction of heat loss from the otherwise large ducting
Disadvantages	➢ High-pressure field piping ➢ Large ducting required ➢ System is difficult to control during insolation transients (especially Rankine) ➢ Extreme care must be taken in the design to prevent tube burnout	➢ Adds complexity and another fluid ➢ Extra heat exchanger

A direct or indirect system can be used in a solar thermal power cycle. For the Brayton cycle, a direct system seems attractive, especially when considering costs. Air can be used as the working fluid in the power cycle and as the fluid which extracts heat from the heat source (solar receiver).

2.2.5 Conclusion

The solar thermal Brayton cycle is recommended over the other solar thermal power cycles by Mills (2004) and Chen et al. (2007). The power cycle uses air as working fluid and has low operation and maintenance costs. When a recuperator is used, the cycle operates at low compressor pressure ratios. Therefore, the solar thermal Brayton cycle is the foundation for the remainder of the literature study.

2.3 Solar collectors (concentrators and receivers)

2.3.1 Background

It is noted from the literature that there is some confusion regarding the definitions of collectors, concentrators and receivers. Duffie and Beckman (1991) take away the confusion regarding these definitions: the *collector* includes the receiver and concentrator, while the *receiver* is the element of the system where the radiation is absorbed and converted into some other energy form. The receiver consists of the absorber, covers and insulation. The *concentrator* is the part of the collector that directs radiation onto the receiver. The concentrator area reflects or concentrates the sun's rays onto the receiver (with the use of reflective material).

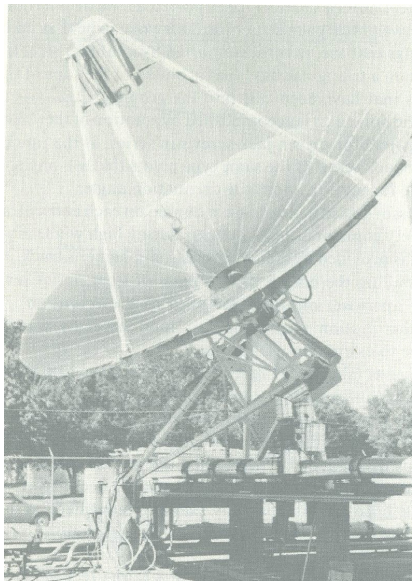

Figure 2.11 Photograph of parabolic dish installed at Shenandoah (Stine and Harrigan, 1985).

The purpose of a solar thermal receiver is to absorb the sun's energy and to transfer the resultant thermal energy to a fluid which, in turn, delivers useful energy (Howell et al., 1982). The method of concentration can be described as the way in which a receiver receives the sun's energy from the concentrator – there are quite a number of different ways in which the sun can be concentrated onto a receiver. The receiver geometry depends on the method of radiation collection. Figure 2.11 shows an example of a small-scale parabolic dish collector, including the concentrator and receiver. According to Duffie and Beckman (1991), many solar power studies showed that the solar collector represents the largest cost in the system.

Literature concerning the basics of solar energy is well established. Kreith and Kreider (1978), Wilson (1979), Howell et al. (1982), Stine and Harrigan (1985) and Duffie and Beckman (1991)

paid much attention to different solar topics. This includes: the sun, history, solar concentrators, flat-plate collectors, energy storage, radiation, sizing, case studies and economics, to name a few. Many of these sources are more focused on solar thermal heating systems than on solar thermal power systems. Stine and Harrigan (1985) paid specific attention to collector performance, basic concentrator optics, parabolic concentrating collectors, central receivers, different types of concentrators and power cycles for solar applications.

2.3.2 Concentration ratio and different types of concentrations

"The higher the temperature at which energy is to be delivered, the higher must be the concentration ratio and the more precise must be the optics of both the concentrator and the orientation system" according to Duffie and Beckman (1991).

Solar collectors can be divided into different classes. Flat plates, which operate without concentration, are regarded as thermal-conversion devices operating over a range of temperatures of up to 380 K (107℃). These collectors are used mainly for service water and space heating (Kreith and Kreider, 1978). Duffie and Beckman (1991) claim that it might be possible to use flat plate collectors to supply energy to heat engines.

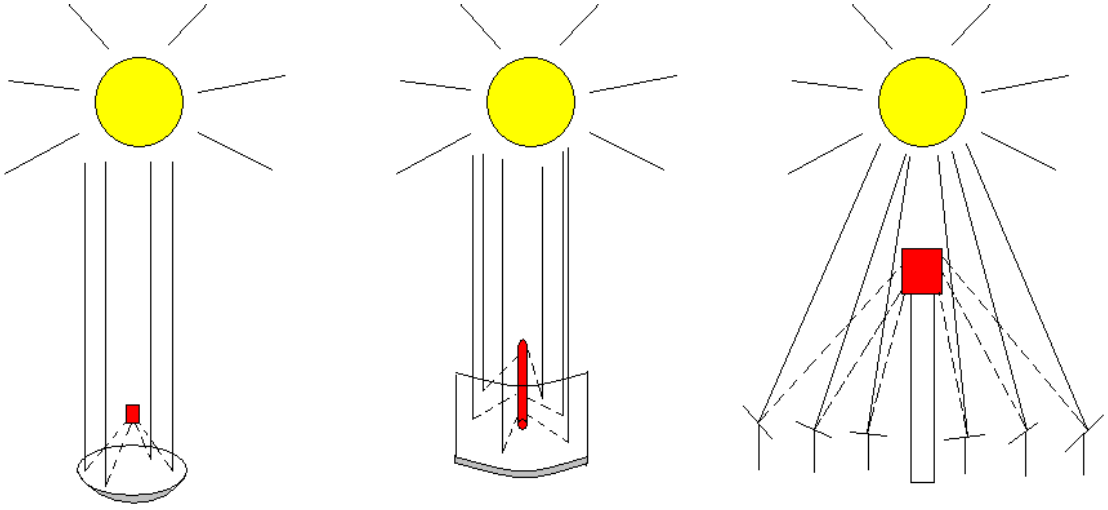

Figure 2.12 Different methods of concentration (dish, trough and tower).

Another group of solar collectors produces very high energy fluxes by accurately tracking the sun (but not always) and by using focusing devices. This is done by using focusing devices connected to a basic absorber-receiver. According to Kreith and Kreider (1978), the highest operating temperatures for concentrated solar power can be as high as 4 000 K. Kreith and Kreider (1978) estimate that the cost of concentrated solar power in the right locations will not be more than that of nuclear power. Figure 2.12 shows the different methods of concentration as dish, trough and

tower. Some other interesting collectors also exist. The hot-line collector uses a wedge-shaped absorber channel and has efficiencies of around 90%. A curved Fresnel lens collector was developed by the Northrup plant in Texas. The compound parabolic concentrator is similar to the natural structure of the eye of the horseshoe crab – one of the most efficient light-gathering structures known (Cheremisinoff and Regino, 1978). Duffie and Beckman (1991) regard honeycombs, compound parabolic concentrators, concentrating collectors and evacuated tubular collectors as recent developments in collector heat loss control or collector efficiency.

Thermodynamic limits to concentration exist. Kreith and Kreider (1978) and Duffie and Beckman (1991) give the theoretical upper limit of concentration for 2D (linear concentration) and 3D concentrators: the maximum linear concentration ratio is in the order of 200, while the maximum 3D concentration ratio is in the order of 40 000. According to Kreith and Kreider (1978), the concentration ratio of single-curvature concentrators (troughs), is usually less than 50, with delivery temperatures of 300°C, while the concentration ratio is higher than 30 and up to several hundreds for double-curvature units. Kreith and Kreider (1978), Stine and Harrigan (1985) and Duffie and Beckman (1991) refer to a *concentration ratio* as the ratio of the net collecting aperture area to the area of the receiver or absorber. Data obtained for solar tower plants by Schwarzbözl et al. (2006) show that the total reflective area divided by the total receiver aperture (or concentration ratio, CR) is on average more or less 700. According to Figure 2.13, a parabolic dish collector should be used when receiver temperatures of between 500 and 1 000°C are required. The shaded area shows the probable range of operation. Figure 2.14 also shows the typical temperatures achievable by concentrating solar collectors.

The high temperatures required for the Brayton cycle would not allow it to be used with troughs. Trough technology cannot reach the high temperatures required. Double-curvature units should be used with a point cavity receiver (Stine and Harrigan, 1985). Figure 2.15 roughly indicates the optimum operating ranges of the different power cycles. A similar figure (Figure 2.16) is given by Wilson (1979) for different concentration optics without a specification of the working fluid used or its mass flow rate.

Figure 2.17 provides another representation of the relationship between fluid temperature and concentration ratio. This figure gives a general guideline of the concentration ratio to be used for a given temperature. The thermal efficiency of the receiver shown in the figure is defined by the ratio of the useful heat to the incoming solar radiation in the receiver aperture. Pitz-Paal (2007) concludes the following from this figure: higher fluid temperatures lead to lower receiver efficiencies, higher concentration factors lead to higher efficiencies and convection and conduction losses are of minor importance at high concentration factors.

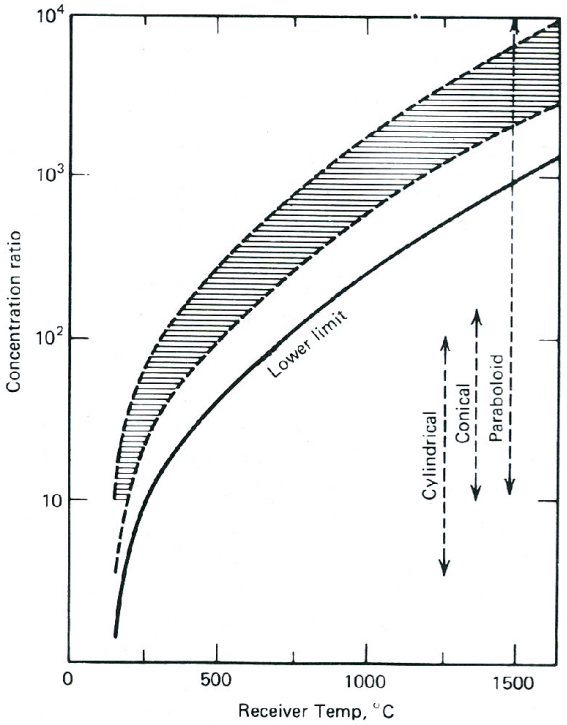

Figure 2.13 Relationship between concentration ratio (area of concentrator divided by the area of receiver) and temperature of receiver operation. The shaded range represents a probable range of operation (Duffie and Beckman, 1991).

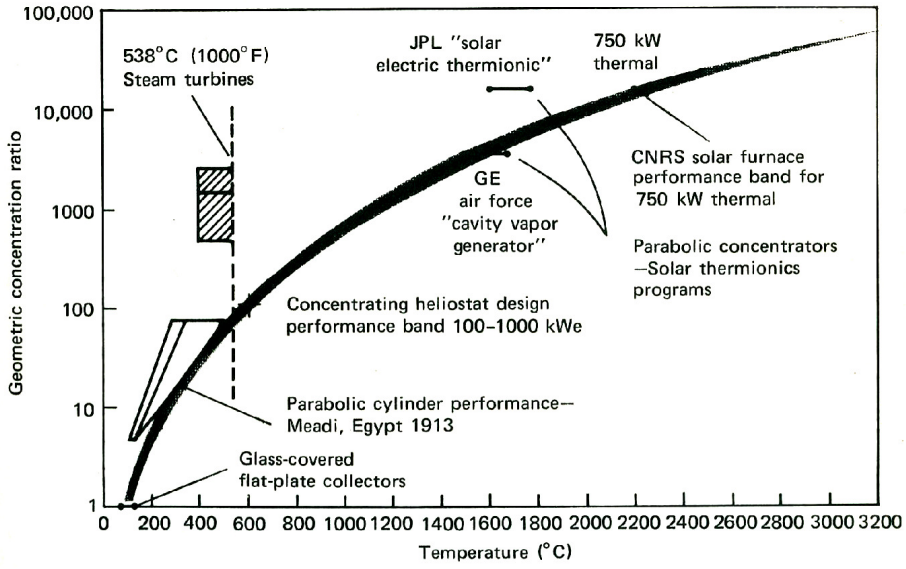

Figure 2.14 Typical temperatures achievable by concentrating solar collectors (Kreith and Kreider, 1978).

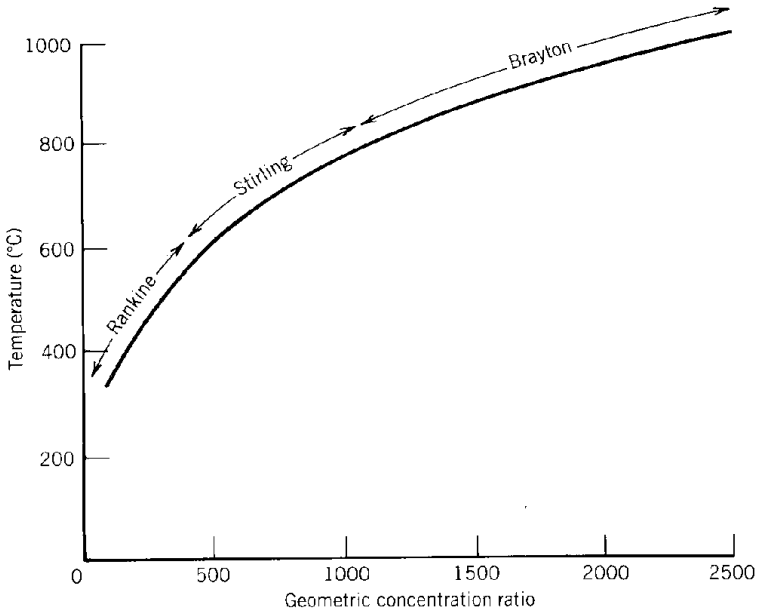

Figure 2.15 Optimum operating temperature change with geometric concentration ratio (Stine and Harrigan 1985).

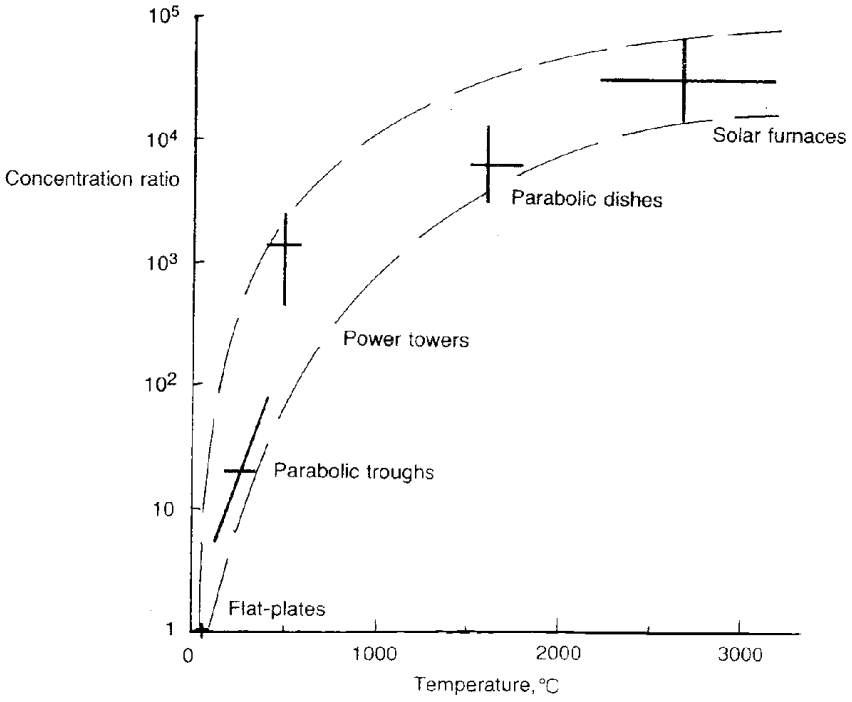

Figure 2.16 Temperature reached by solar absorbers using concentration optics (Wilson, 1979).

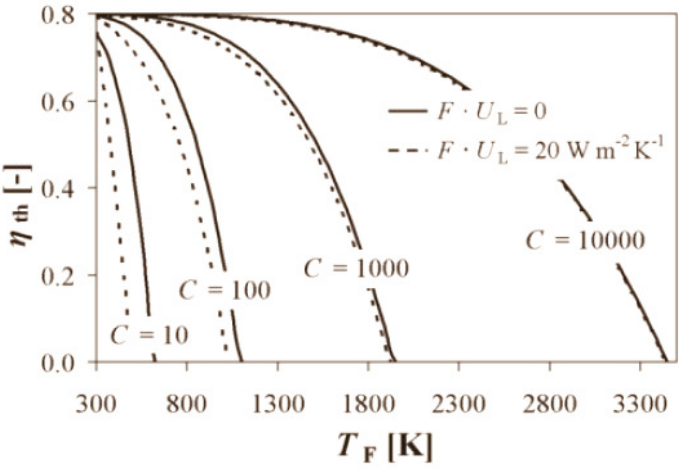

Figure 2.17 The thermal efficiency of a receiver as a function of the fluid temperature and the concentration factor (Pitz-Paal, 2007).

Figures 2.18 and 2.19 conclude that selective absorber properties significantly increase a receiver's performance, specifically in the case of low concentrating systems and high temperatures. In practice, however, selective coatings are only available up to a temperature of about 800 K, so that selective coatings are irrelevant for high-temperature solar concentrators. Pitz-Paal (2007) suggests that a possible solution is the use of a cavity receiver. The concentrated radiation enters through a small aperture in a thermally insulated cavity. The actual absorbers are distributed on the inner-cavity walls (Pitz-Paal, 2007).

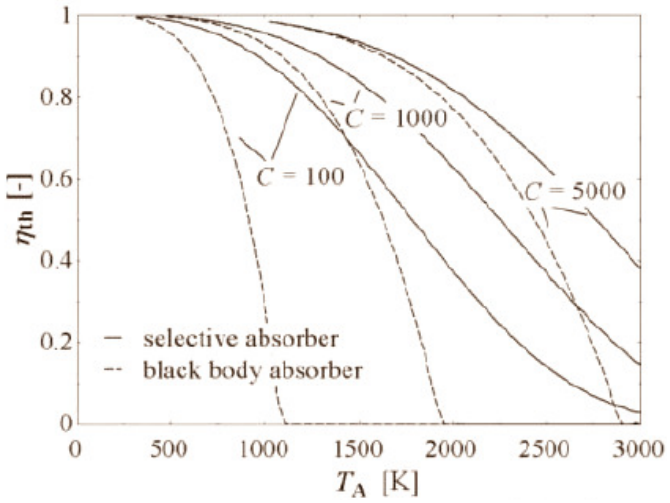

Figure 2.18 The thermal efficiency of a receiver as a function of the absorber temperature and the concentration factor. The use of a selective absorber and a blackbody absorber is considered. Convection heat losses are neglected (Pitz-Paal, 2007).

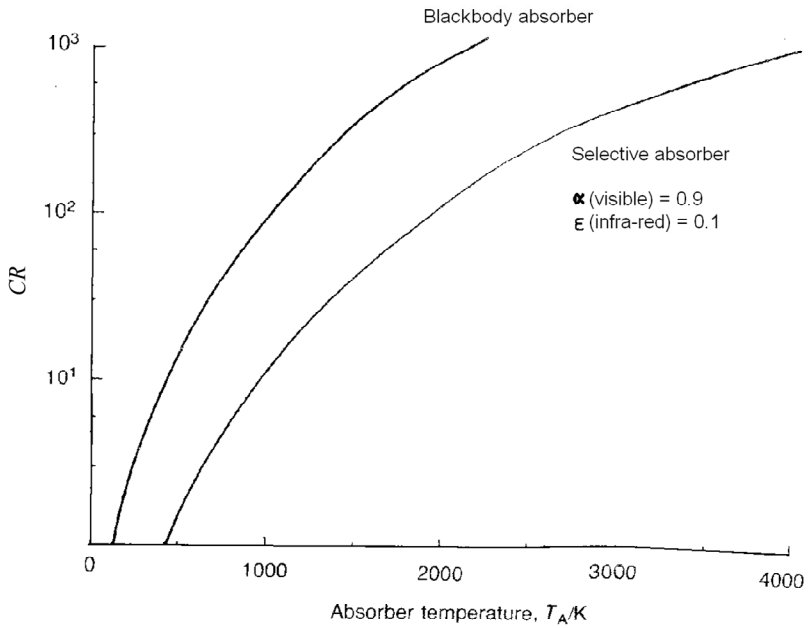

Figure 2.19 Expected stagnation temperatures of evacuated solar collectors with concentrators, where α and ε describe the properties of the selective absorber (Wilson, 1979).

Bejan (1997) found that the optimisation of a collector and engine arrangement can consist of selecting not only the collector temperature but also the cut-off frequency. Omnicolour series of ideal concentrators were evaluated and it was found that it improved only slightly on the maximum work per area ratio (Bejan, 1997).

2.3.3 Rim angle, tracking and solar irradiation

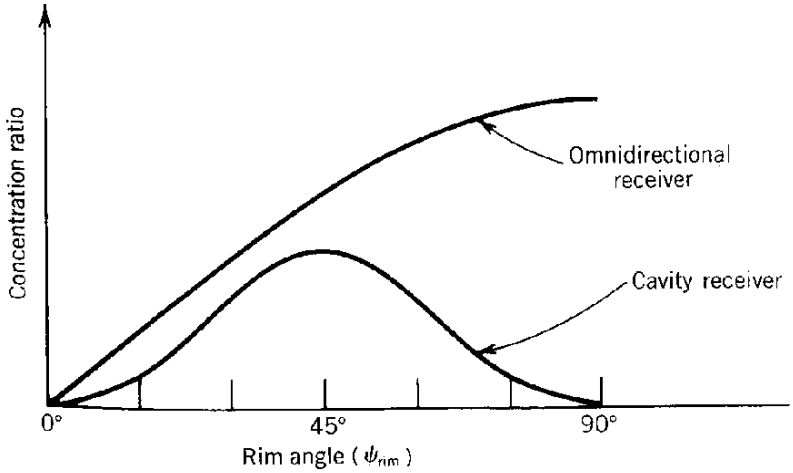

Figure 2.20 Variation of geometric concentration ratio with rim angle (Stine and Harrigan, 1985).

According to Stine and Harrigan (1985), a rim angle of 45° (Figure A.2 in Appendix A, schematically shows the definition of the parabolic dish concentrator rim angle) gives the

maximum concentration ratio for a parabolic dish collector. This is shown in Figure 2.20. This figure also includes the curve for the omnidirectional receiver. Only the trends of these curves are shown and their magnitude relative to each other is not correct.

Concentrated solar thermal power systems usually require tracking of the sun. Two different tracking levels exist: intermittent tilt change or completely fixed and continuously tracking, which is used for high concentration ratios (Duffie and Beckman, 1991). The acceptance angle of focusing collectors decreases with increasing concentration ratio. Stine and Harrigan's (1985) research shows that two-axis tracking can be regarded as the best available tracking method, as shown in Figures 2.21 and 2.22. Focusing collectors must track the sun with a degree of precision that increases with the concentration ratio. If a solar collector moves with two degrees of freedom, it can track the sun at zero incidence angle throughout the day to intercept the maximum amount of beam radiation (Kreith and Kreider, 1978). For the solar thermal Brayton cycle, two-axis tracking will be required.

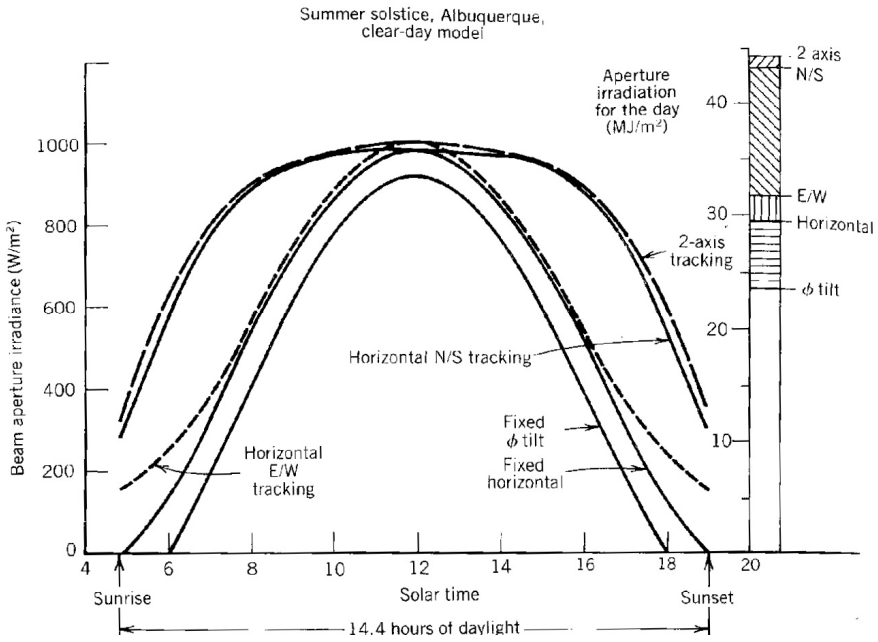

Figure 2.21 Aperture irradiance for different fixed and tracking aperture configurations for Albuquerque, on June 22 (Stine and Harrigan, 1985).

Direct, diffuse and reflected radiations are mentioned as the three different components of solar radiation (Cheremisinoff and Regino, 1978). According to Stine and Harrigan (1985), the radiation falling directly on the earth is 451 – 1 135 W/m^2. The irradiance of Albuquerque (New Mexico, US) can be as high as 1 000 W/m^2 and as low as 500 W/m^2 at noon through summer and winter for different types of tracking methods. Kreith and Kreider (1978) give a value of 300 W/m^2 (in the Red Sea area) as the highest annual mean irradiance (amount of solar radiant energy falling on a

surface per unit area and per unit time). According to Fluri (2009), the solar irradiation in the northern parts of the Northern Cape Province, South Africa, is more than 8 kWh/m^2 in December and 6 kWh/m^2 in June. Most areas in South Africa, however, receive an average of more than 2 500 hours of sunshine per year, with average solar-radiation levels ranging between 4.5 and 6.5 kWh/m^2 per day (DME, 2010). For a steady-state analysis, 1 000 W/m^2 would be an acceptable value for a high irradiance location in South Africa, at noon.

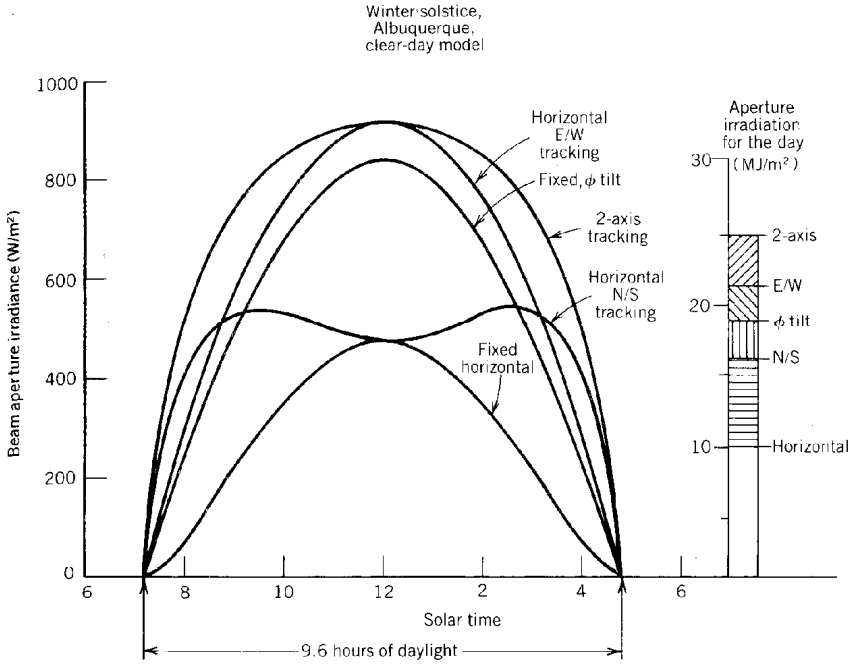

Figure 2.22 Aperture irradiance for different fixed and tracking aperture configurations for Albuquerque, on December 22 (Stine and Harrigan, 1985).

2.3.4 Losses and efficiency

From the literature, it is clear that there are many different collector efficiencies available, each defined differently. According to Howell et al. (1982), there exists a solar collector efficiency (due to inefficiencies in the reflective process). According to Stine and Harrigan (1985), losses associated with reflection typically range from about 5 to 25% and other optical losses that occur in a concentrating collector are transmittance and receiver absorptance. They also mention that a glass cover, which can be used to reduce the convective losses from the receiver, can absorb about 5% of the light energy passing through it. Figure 2.23 shows the specular reflectance of aluminium, silver and gold. Stine and Harrigan (1985) emphasise the importance of good thermal contact between receiver and working fluid, evacuated annulus between glass cover and receiver, a receiver mounted in a cavity (to reduce convection losses) and selective coating for reducing the thermal losses due to radiation. High-absorptance paint has an absorptance of 0.95.

If the absorbing surface is inside a cavity, the effective absorptance increases to about 0.98 (Stine and Harrigan, 1985).

It is clear that collector efficiencies are defined differently. There has yet been no mention of entropy generation in collectors and solar thermal power systems, or the second law of thermodynamics, which would be the focus of this study. A comprehensive section on the second law and the solar thermal Brayton cycle is given in Section 2.6.

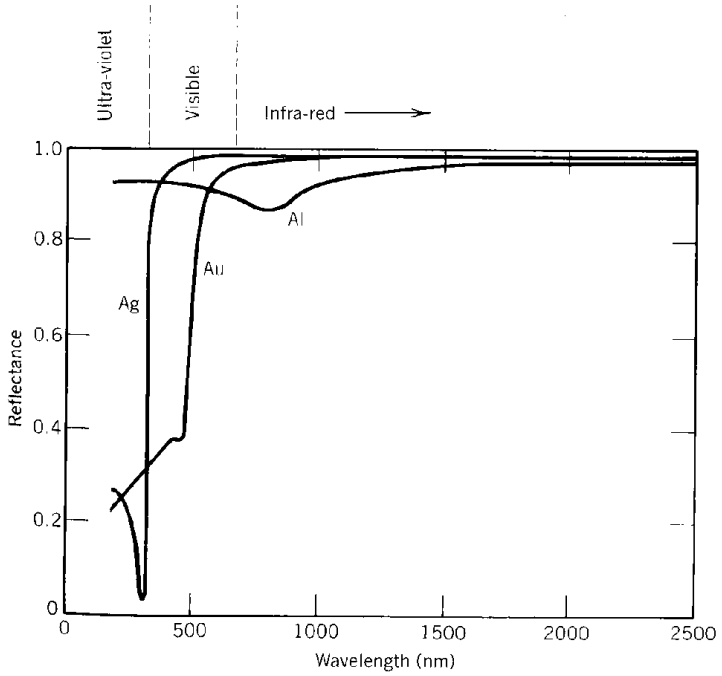

Figure 2.23 Specular reflectance of selected materials: silver, aluminium and gold (Stine and Harrigan, 1985).

2.3.5 Solar receivers

According to Stine and Harrigan (1985), if a black receiver is mounted at the focus of a parabolic dish reflector, the reflected light will be absorbed and converted into heat. According to Bejan (1997), the solar receiver can be viewed as a blackbody that is exposed to blackbody radiation of a higher temperature (as a first-cut model). For the Brayton cycle, large receivers are required due to the low gas heat transfer coefficients (Duffie and Beckman, 1991). Parabolic concentrators reflect light either to a point or a line. The solar receiver intercepts the energy available at this point or line. There are only two widely used receivers: the linear omnidirectional receiver and the point cavity receiver or focal plane receiver. The point cavity receiver can also be used with a parabolic trough when the cavity is linear, but it is commonly used with parabolic dishes (Stine and Harrigan, 1985). The convection and radiation losses are drastically reduced when a receiver is mounted in a cavity with a selective coating. Other types of solar receivers are also found.

Bertocchi et al. (2004) describe the heating of air temperatures to far more than 1 000℃, using a high-temperature solar particle receiver. Heller et al. (2006) demonstrate that volumetric pressurised receivers are able to produce air of 1 000℃ to drive a gas turbine. These receivers are more complex and expensive.

The performance of different cavity receivers was investigated by Shuai et al. (2008), Prakash et al. (2009) and Sendhil Kumar and Reddy (2008). Figure 2.24 shows a typical cavity receiver. According to Pitz-Paal (2007) the inherent characteristic of a cavity receiver aperture is that a blackbody is approximated.

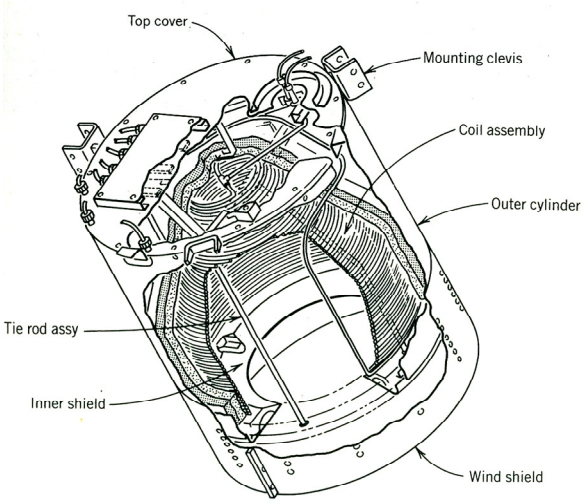

Figure 2.24 A typical cavity receiver (Stine and Harrigan, 1985).

The thermal losses of a cavity receiver include convective and radiative losses to the air in the cavity, as well as conductive heat loss through the insulation used behind the helical tube surface. Shuai et al. (2008) investigated different classical cavity geometries and found that cavity geometry has a significant effect on overall distribution of radiation flux in the cavity receiver. According to Shuai et al. (2008), an upside-down pear cavity might be a desirable shape. Prakash et al. (2009) investigated heat losses from a solar cavity receiver at different inclination angles, with head-on and side-on winds. According to Prakash et al. (2009), the thermal and optical losses occurring from an open-cavity solar receiver are less when compared with other types of receivers and, hence, such receivers are preferred.

Reddy and Sendhil Kumar (2008) compared different types of cavity receivers numerically and found that their modified cavity receiver experienced lower convection heat losses than those of the other receivers and suggested that it may be preferred in a solar dish collector system. A numerical investigation of natural convection heat loss (Sendhil Kumar and Reddy, 2007), an

investigation of the contribution of radiation losses (Reddy and Sendhil Kumar, 2008) and an improved model for natural convection heat loss were presented for the modified cavity (Reddy and Sendhil Kumar, 2009). Figure 2.25 shows the modified cavity receiver.

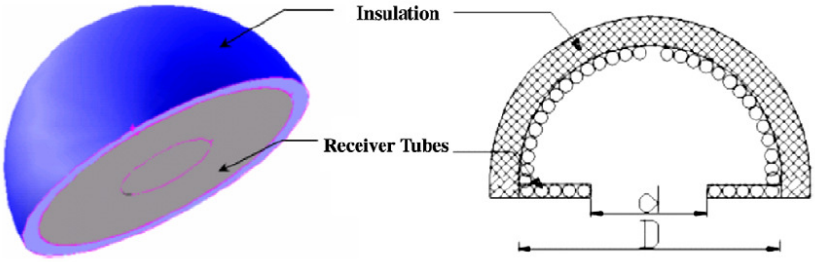

Figure 2.25 Modified cavity receiver (Reddy and Sendhil Kumar, 2009).

Sendhil Kumar and Reddy (2008) suggest the use of their modified cavity receiver with an area ratio of

$$A_w / A_a = 8 \tag{2.1}$$

where A_w is the inner-surface area of the cavity and A_a the aperture area. This area ratio gives the minimum heat loss. Figure 2.26 shows this cavity receiver.

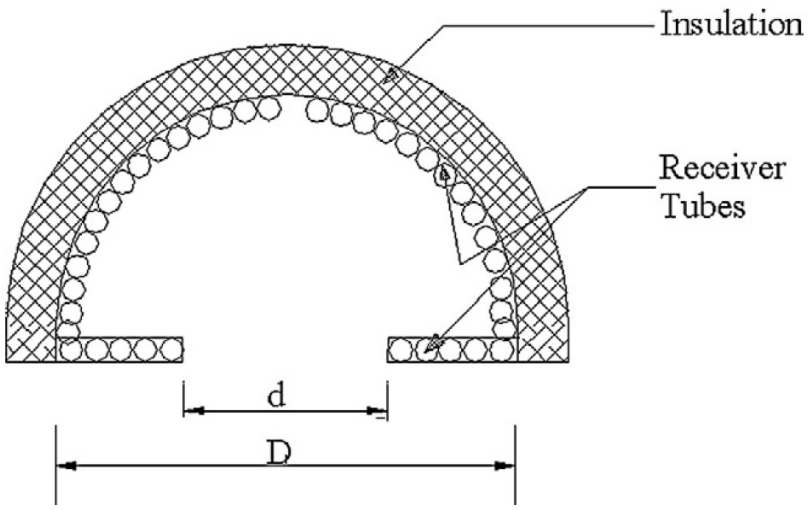

Figure 2.26 Modified cavity receiver (Reddy and Sendhil Kumar, 2008).

The areas of the aperture and the inner wall can be calculated with the following equations respectively:

$$A_a = \frac{\pi d^2}{4} \tag{2.2}$$

and

$$A_w = \frac{3\pi D^2}{4} - A_a \tag{2.3}$$

For a specific concentrator diameter (with constant focal length and rim angle), the net rate of heat absorbed by the working fluid in the receiver depends on the receiver aperture diameter. The sun's rays are not truly parallel and concentrator errors exist, which means that the reflected rays form an image of finite size centred around the focus, instead of a focal point.

Thus, the geometry of a cavity receiver can determine the amount of heat available to be transferred to the working fluid. A receiver can be optimally sized, since the aperture area of the solar receiver will determine the amount of heat intercepted, but also the amount of heat lost due to convection and radiation. The larger the cavity aperture, the more heat can be intercepted, but also the more heat can be lost due to convection and radiation (Stine and Harrigan, 1985). For a fixed dish concentrator area, the amount of heat available for the working fluid, which is the intercepted heat absorbed minus the heat lost due to radiation and convection, is a function of the cavity aperture diameter.

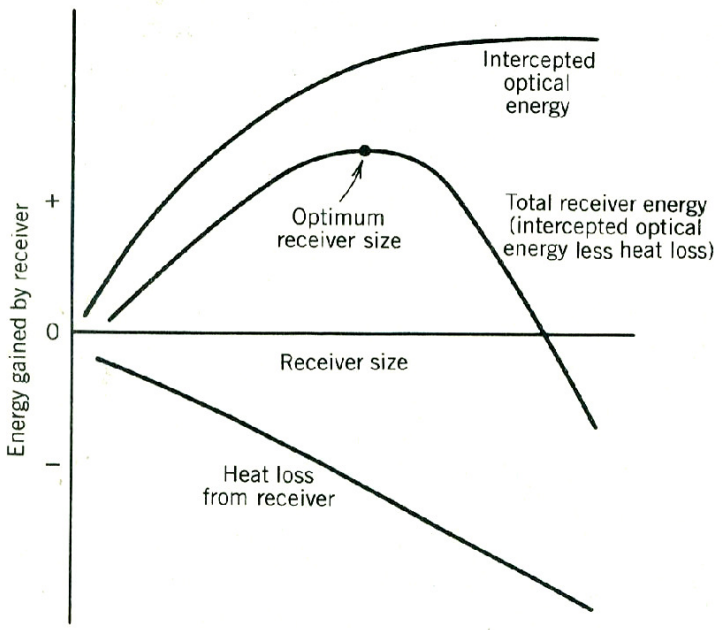

Figure 2.27 Sizing of a collector receiver (Stine and Harrigan, 1985).

Figure 2.27 shows the sizing of receivers in general. There exists a cavity aperture area which allows the maximum net absorbed heat. Steinfeld and Schubnell (1993) present a semi-empirical method to determine the optimum aperture size and optimum operating temperature of a solar cavity receiver, which has a maximum energy conversion efficiency. Figure A.1 in Appendix A, shows the logical flow for a receiver sizing algorithm of Stine and Harrigan (1985) which can be used with a fixed dish concentrator area to get the amount of energy available (intercepted) for a specific cavity aperture area. Appendix A explains the method in which the algorithm is used.

Narendra et al. (2000) believe it is important that extensive work is carried out in the field of material constraints to make solar thermal power a real success because the material constraints of the solar receiver play an important role in exergy loss. This is because the high quality solar energy is used to heat the fluid at a much lower temperature due to the temperature constraint. It is thus important to know what the maximum or melting surface temperature of the receiver could be. This depends on the material used. The melting temperature of copper is 1 084 °C / 1 357 K. According to the Copper Tube Handbook (Copper Development Association, 2006), standard brazing fluxes can protect up to temperatures of 871 °C / 1 144 K and special brazing fluxes up to 1038 °C / 1 311 K.

Thus, a cavity receiver (which can withstand high temperatures) should be used for the solar thermal Brayton cycle. A receiver aperture sizing algorithm should be used to determine the available heat for the power cycle. A heat loss model for the modified cavity receiver is available (Reddy and Sendhil Kumar, 2009).

2.4 Heat exchangers in general and the recuperator

Heat exchangers are required to be efficient, economical, safe, simple and convenient (Yilmaz et al., 2001). Heat transfer and pressure losses as well as the optimisation of size, weight and price should be taken into consideration while the heat exchanger is being designed (Oğulata et al., 2000). According to Bejan (1982), heat exchanger irreversibilities can be reduced by slowing down the movement of fluid through the heat exchanger which is synonymous with employing larger heat exchangers. The irreversibility of a fixed-area heat exchanger can be reduced by properly distributing or arranging the area (Bejan, 1982).

A recuperator (heat exchanger) can be used in the Brayton cycle (Figure 2.4) to extract the heat from the turbine outlet and transfer it to the cold stream before it is heated by the heat source. Kreith and Kreider (1978) suggest that counterflow heat exchangers should be used in solar thermal power systems and parallel-flow heat exchangers should be avoided. They suggest the

use of a heat exchanger penalty, which decreases as heat exchanger effectiveness increases. According to data given by Çengel (2006), it is concluded that the most effective heat exchanger is a counterflow heat exchanger. Bejan (1982) mentions that counterflow heat exchangers find numerous applications in recuperative heating associated with the Brayton cycle. The definitions used for the terms *recuperator efficiency*, according to Çengel (2006), and *effectiveness*, according to Stine and Harrigan (1985), are the same.

Shah (2005) suggests that counterflow plate-type heat exchangers can be used as compact recuperators with micro-turbines. Shah (2005) gives design criteria for micro-turbine recuperators. Some of these criteria are high performance with minimum cost, high exchanger effectiveness, compactness, 40 000 hour operation life without maintenance, low pressure loss (< 5%). According to Shah (2005), the abovementioned criteria translate into a thin foil primary surface recuperator (same surface on both fluid sides) with stamping, folding and welding side edges by an automated operation to form flow passages.

2.5 Summary of literature in Sections 2.2 to 2.4

With the aid of the preceding literature, a few observations were made regarding the solar thermal Brayton cycle, its collector and its recuperator. The open and direct solar thermal Brayton cycle with recuperator, cavity receiver and micro-turbines from Garrett will be used in the analysis. A counterflow plate-type recuperator will be beneficial. A maximum receiver temperature should be specified due to material constraints. The following collector scheme was identified for the power cycle: a parabolic dish concentrator with 45° rim angle, modified cavity receiver, two-axis tracking, concentrator reflectance > 90% and an average irradiance of 1 000 W/m^2.

2.6 The second law of thermodynamics

2.6.1 Background

The second law of thermodynamics is the set of rules which governs all changes occurring in nature. It is an unfortunate case that it is not used enough in design (Sama, 1995). “The first law of thermodynamics states that a certain energy balance will hold when a system undergoes a change of state or a thermodynamic process, but it does not give any information on whether that change of state or the process is at all feasible or not” according to Oğulata et al. (2000). An analysis based on the second law of thermodynamics is necessary for determining the maximum net power output of a solar thermal Brayton cycle.

Shiba and Bejan (2001) regard exergy analysis, irreversibility minimisation, entropy generation minimisation or thermodynamic optimisation and thermoeconomics as the most established

changes in methodology experienced in engineering thermodynamics during the 1980s to 2000. Bejan et al. (1996) present the current status of exergy analysis, EGM (entropy generation minimisation) and thermoeconomics. According to Shiba and Bejan (2001), at the beginning of the 21st century, the focus of engineering thermodynamics was on identifying the mechanisms and system components responsible for thermodynamic losses, as well as the minimisation of these losses subject to global constraints on the system. This includes the minimisation of costs associated with building and operating the energy system.

Bejan (1982) states that the long-term answers to energy questions must rest on a solid thermodynamic foundation and the second law, in particular, should occupy a central place in heat transfer thought. Entropy generation minimisation, according to Bejan (1982), should bridge the gap between three cornerstone subjects: heat transfer, thermodynamics and fluid mechanics. The topic of irreversibility and availability is well covered by Sonntag et al. (2003). In an ideal system, there would be no entropy generation (no irreversibilities). Optimisation studies were carried out for such solar thermal power plants (reversible systems) where the irreversibilities are neglegted. Bejan (1997), for example, optimised a reversible extraterrestrial solar power plant, which was purely focused on radiation heat transfer only. It was found that the receiver area should be about half the size of the radiator area.

Effects which cause irreversibilities, according to Bejan et al. (1996) and Sonntag et al. (2003), are heat transfer through a finite temperature difference, unrestrained expansion of a gas or liquid to a lower pressure, spontaneous chemical reaction, mixing of matter at different compositions or states, friction such as sliding friction as well as friction in the flow of fluids, electric current flow through a resistance, magnetisation or polarisation with hysteresis, and inelastic deformation.

These irreversibilities can be divided into two classes: internal (occurring within a system) and external (occurring within the surroundings). Irreversibilities related to friction, unrestrained expansion and mixing can be regarded as secondary in importance to those of combustion and heat transfer. The irreversibilities of convective heat transfer are due to heat transfer across a non-zero temperature difference and fluid friction (Bejan, 1982; Bejan et al., 1996).

Zimparov et al. (2006a) state that to improve the global thermodynamic performance of a system, “the irreversibilities (entropy generation or exergy destruction) that characterises all the components and processes of the system, must be decreased”. This is done “by spreading the entropy generation rate through the system in an optimal way, by properly sizing, shaping and positioning components” according to Zimparov et al. (2006c).

2.6.2 Exergy

Exergy, or availability, has become an increasingly important tool for the design and analysis of thermal systems since it correctly reveals the principle sites of thermodynamic inefficiencies, owing to irreversibilities. *Exergy* is defined as the maximum theoretical useful work obtainable, as two systems at different states interact to equilibrium (when one of the systems is the environment), with heat transfer occurring with the environment only. Natural resources can be seen as availability reserves (oil, coal, uranium, etc.). The more irreversibilities one has when using these reserves, the greater will be the decrease in availability and the greater the decease in natural reserves (Sonntag et al., 2003). Exergy can thus be destroyed and it can never be negative (Bejan et al., 1996).

2.6.2.1 Closed-system exergy balance

Equation 2.4 shows a closed-system exergy balance (Bejan et al., 1996). From this equation, the following can be concluded: the total number of exergy transfers (into a system) is split up into two parts - the making of an actual exergy change in the closed system between two states and the destruction of exergy (which is a direct function of entropy generation, as shown in the Gouy-Stodola theorem, equation 2.5). Exergy destruction is also known as availability destruction, the irreversibility and the lost work:

$$\left(E_2 - E_1\right) = \int_1^2 \left(1 - \frac{T_0}{T_b}\right)\delta Q - \left[W - p_0\left(\upsilon_2 - \upsilon_1\right)\right] - T_0 S_{gen} \tag{2.4}$$

$$E_D = T_0 S_{gen} \tag{2.5}$$

It can be concluded that:
Exergy Change = Exergy Transfers - Exergy Destruction.

The exergy transfers in the closed-system exergy balance are split into the exergy transfers associated with the transfer of energies by heat transfer and by work. From equation 2.4 it follows that the work into a system will be regarded as a positive exergy transfer into the system, since the work into a system is regarded as negative. This makes sense since exergy, or available work, should increase when work is put into the system, as opposed to work input, which is regarded as negative, from an energy perspective.

Exergy can also be divided into four components (equation 2.6): physical (function of pressure and temperature), kinetic (function of velocity), potential (function of height) and chemical exergy (not shown in equation 2.6):

$$E_2 - E_1 = (U_2 - U_1) + p_0(V_2 - V_1) - T_0(S_2 - S_1) + (KE_2 - KE_1) + (PE_2 - PE_1) \quad (2.6)$$

The equation for internal energy change (equation 2.7), can be compared with the equation for exergy change (equation 2.6) to show the difference between energy and exergy:

$$(U_2 - U_1) = Q - W - (KE_2 - KE_1) - (PE_2 - PE_1) \quad (2.7)$$

2.6.2.2 Exergy balance for control volumes

Equation 2.8 shows the exergy balance concept extended to a control volume (Bejan et al., 1996; Sonntag et al., 2003), which is more practical. The definitions for specific exergy transfers at inlets and outlets are given in equation 2.9 (Bejan et al., 1996):

$$\frac{dE_{cv}}{dt} = \sum_j \left(1 - \frac{T_0}{T_j}\right)\dot{Q}_j - \left(\dot{W}_{cv} - p_0 \frac{dv_{cv}}{dt}\right) + \sum_i \dot{m}_i e_i - \sum_e \dot{m} e_e - \dot{E}_D \quad (2.8)$$

where

$$e = (h - h_0) - T_0(s - s_0) + \tfrac{1}{2}V^2 + gz + e^{CH} \quad (2.9)$$

against

$$\hat{e} = u + \tfrac{1}{2}V^2 + gz \quad (2.10)$$

The difference between the specific exergy and specific energy can be identified by comparing equations 2.9 and 2.10 respectively (Bejan et al., 1996). Exergy is concerned with giving values from differences between a certain point and the environment while energy is not concerned with its magnitude relative to the environment. The other two terms (concerning velocity and height) stay the same, since velocity's reference point is already zero and height can simply be seen as a distance, regardless of the reference point (although a practical reference point for height in the exergy equation could be sea level). This seems to be the intrinsic difference between energy and exergy: the fact that exergy, unlike energy, uses the environment as its reference point for all

of its components. The exergetic approach seems to be more practical since humans are situated in this environment and one would like to know what the optimal possibilities are for inhabitants of this environment instead of inhabitants of infinite space.

2.6.2.3 Exergetic efficiency

According to Bejan et al. (1996), exergetic efficiency (second law efficiency, effectiveness or rational efficiency) is a parameter for evaluating thermodynamic performance. It provides a true measure of the performance of an energy system from a thermodynamic viewpoint. It is necessary to identify both a product and a fuel for the thermodynamic system being analysed (equation 2.11). Bejan et al. (1996) identify these exergy rates associated with a fuel and product for the compressor, turbine, heat exchanger, mixing unit, combustion chamber and boiler at steady-state. Sonntag et al. (2003) have a similar approach to the efficiency of a heat exchanger, as will be shown later in equation 2.15.

$$\varepsilon = \frac{\dot{E}_P}{\dot{E}_F} = 1 - \frac{\dot{E}_D + \dot{E}_L}{\dot{E}_F} \tag{2.11}$$

According to Bejan et al. (1996), the exergetic efficiency is generally more meaningful and useful than any other efficiency based on the first or second laws of thermodynamics, including the thermal efficiency of a power plant, isentropic efficiency of a compressor or turbine and effectiveness of a heat exchanger. Yilmaz et al. (2001) summarise the interrelations of performance criteria for both exergy and entropy analysis. The exergetic efficiency or second law efficiency, which gives an indication of the degree of thermodynamic perfection, is regarded as of little use for individual plants and units such as heat exchangers and it is stated that it may even lead to false conclusions.

2.6.3 Entropy

Equation 2.12 (second law of thermodynamics) expresses the change of entropy for an irreversible process. According to Sonntag et al. (2003), entropy increase is the change from a less probable to a more probable state and the entropy of a system can be increased in two ways: by transferring heat to it and by having an irreversible process. For the entropy change of an ideal gas, equation 2.13 (Sonntag et al., 2003) can be used with constant specific heat. Consider the design of lifting a weight with a rope. Entropy generation is proportional to additional work wasted for a bad lifting design (Bejan, 1982). Entropy generation can be minimised:

$$S_2 - S_1 = \int_1^2 \frac{\partial Q}{T} + S_{gen} \tag{2.12}$$

$$s_2 - s_1 = c_{p0} \ln \frac{T_2}{T_1} - R \ln \frac{P_2}{P_1} \tag{2.13}$$

From the second law (equation 2.12) follows that only the heat transfer, not work transfer interactions, is accompanied by entropy transfer (Bejan, 1982). Entropy generation is path-dependent and not a thermodynamic property and should not be confused with the thermodynamic property entropy change ($S_2 - S_1$). According to Bejan et al. (1996), the direction of the entropy transfer is the same as that of the heat transfer. Equation 2.14 (Sonntag et al., 2003) gives the expression for the balance of entropy for a control volume:

$$\frac{dS_{cv}}{dt} = \sum \dot{m}_i s_i - \sum \dot{m}_e s_e + \sum \frac{\dot{Q}_{cv}}{T} + \dot{S}_{gen} \tag{2.14}$$

The Gouy-Stodola theorem (equation 2.5) states that the lost available work is directly proportional to the entropy generation in a system (Bejan, 1982; Bejan, 1997; Bejan et al., 1996). Lost available work is a relative quantity that depends on the choice of reference heat reservoir (Bejan, 1982).

Bejan (1982) provides a number of features most guilty of entropy generation (similar to the features guilty of irreversibilities): heat transfer across a non-zero temperature difference, flow with friction, mixing, filling and discharge, compression, expansion and combustion. The overall irreversibility of compression and expansion (in compressors and turbines), is described by the compressor and turbine efficiencies (Bejan, 1982). The definition of these efficiencies is available from Dixon (2005). Bejan et al. (1996) considered the simultaneous effect of heat transfer and fluid friction on entropy generation and showed that they tend to compete with one another when a thermodynamic optimum is needed.

2.6.4 Second law optimisation and examples of entropy generation minimisation (EGM) for individual components and elemental features

The method of entropy generation minimisation is based on equations used to describe entropy generation mechanisms. Appendix B summarises the relevant entropy generation equations available from the literature. A summary of the following literature and its relevance for the solar thermal Brayton cycle is given in Section 2.6.7.

2.6.4.1 Background

In the field of heat transfer, optimisation is mostly carried out at two levels of complexity: optimisation of complete components like heat exchangers and elemental features like fins and ducts. Heat transfer design objectives can be categorised into two large categories: heat transfer augmentation (conductance) problems and thermal insulation problems. In both cases, EGM is the hidden consequence of good engineering thinking applied to both problems. EGM should close the gap between heat transfer and thermodynamics. EGM has shown that optima exist when the thermodynamic optimisation is subjected to finite-size and finite-time constraints (Bejan, 1982; Bejan, 1996).

The following synonyms can be given for EGM: thermodynamic optimisation, finite-time thermodynamics, second law analysis, thermodynamic design, endoreversible thermodynamics and exoirreversible thermodynamics. The field of EGM experienced astonishing growth during the 1980s and 1990s in both engineering and physics. The EGM method relies on the simultaneous application of heat transfer and engineering thermodynamics principles in the pursuit of realistic models, which account for the inherent thermodynamics irreversibility of the heat, mass and fluid flow processes for heat transfer processes, devices and installations (Bejan, 1996).

The first power generation area to use EGM models regularly was that of solar-driven power plants. It was found that, for a solar receiver with convective heat loss, an optimum coupling between the receiver and the power cycle exists, so that the power output is a maximum. The thermodynamic trade-offs can be of two kinds: when an overall size constraint exists, there is an optimal way of allocating the hardware between the different components, while, for a known daily variation of solar heat input, an optimal time-dependent strategy of plant operation exists (Bejan, 1996; Bejan, 1997).

Yilmaz et al. (2001) imply that engineering thermodynamics includes three important types of approaches based on the second law: EGM, exergy analysis and thermoeconomics. Losses due to process irreversibility can be calculated using a second law analysis. According to Yilmaz et al. (2001), the selection of entropy measure as evaluation parameter, rather than exergy measure, has several advantages. Different entropy evaluation parameters are available from Yilmaz et al. (2001): the entropy generation number, augmentation entropy generation number, heat exchange irreversibility norm, Witte-Shamsundar efficiency and the local entropy generation number. These entropy evaluation parameters are mostly used in the literature to perform optimisation with. It works well for EGM of specific individual components.

In the literature, there are many differently defined entropy generation numbers. Yilmaz et al. (2001) present all the different non-dimensional entropy generation numbers, of which the most frequently used number is the number obtained when the entropy generation rate is divided by the capacity flow rate. Very useful references are available from Yilmaz et al. (2001) for optimisation based on entropy generation numbers, for the following heat exchangers: balanced and unbalanced counterflow heat exchangers, cross-flow heat exchangers, external flow heat exchange (like fins), two-phase flow heat exchangers, regenerative heat exchangers, plate-type heat exchangers and shell-and-tube heat exchangers. The entropy generation numbers, or non-dimensionalised entropy generation equations, are used widely in the literature to minimise entropy generation for individual components or elemental features. These equations are based on entropy generation equations, which are available in Appendix B.

2.6.4.2 Applications

2.6.4.2.1 Internal flow

EGM has been applied for internal flow for constant heat flux or constant wall temperature and different cross-sectional shapes. Bejan (1982) and Bejan et al. (1996) determined the optimum tube diameter or Reynolds number for a tube with internal flow using EGM. Ratts and Raut (2004) also determined the optimal Reynolds number for single-phase, fully developed, laminar and turbulent flow with constant heat flux using EGM. They also compared optimal Reynolds numbers and minimum entropy generation for different cross-sections (circular, square, rectangle and equilateral triangle). Ratts and Raut (2004) found that, for the same deviation from optimal Reynolds number in laminar and turbulent flow, the increase in entropy generation is smaller for heat dissipation than for viscous dissipation. A rectangle with an aspect ratio of eight gives the minimum entropy generation in laminar flow and turbulent flow (Ratts and Raut, 2004). Zimparov et al. (2006a; 2006b; 2006c) did the optimisation of various flow geometries using the entropy generation method and assumptions of constant wall temperature or constant heat flux.

2.6.4.2.2 External flow

The length of a plate is the only design variable capable of inducing changes in the rate of entropy generation in external flow. An optimum plate length exists so that the entropy generation rate reaches a minimum, according to Bejan (1982). This result is important in the local optimisation of plate-finned surfaces in heat exchangers. There is competition between heat transfer and fluid mechanics terms to get an optimal body size with minimum entropy generation (Bejan, 1996; Bejan, 1982; Bejan et al., 1996).

2.6.4.2.3 Augmentation techniques

Various authors investigated heat transfer augmentation techniques using an entropy generation analysis. Roughened surfaces, promoters of swirl flow and fins were considered by Bejan (1982). It was found that the use of twisted tape inserts can lead to savings in exergy and that an optimum fin geometry exists, for which the balance between thermal contact irreversibility and fluid drag irreversibility leads to an overall minimum rate of entropy generation. Zimparov (2001) investigated heat transfer enhancements in tubes using a second law analysis, to display inappropriate enhanced surfaces and assist the engineer in designing better heat transfer equipment. Yilmaz et al. (2001) presented various methods which evaluate heat transfer enhancement techniques.

2.6.4.2.4 Local entropy generation

According to Bejan (1996), several authors recommended that commercial computational fluid dynamics packages should have a built-in capacity of displaying local entropy generation rate in both the laminar and turbulent flow regimes. Bejan (1982) presents the entropy generation rate per unit volume and the entropy generation profile or map for Poiseuille flow through a round smooth tube. According to Bejan (1982), the fluid friction irreversibility term is usually neglected in the first law but it is not necessarily negligible in the entropy generation equation.

There are several advantages to evaluating entropy generation in a local sense. In order to determine the entropy generation rates, the coupled momentum and energy equations should be solved. The corresponding entropy generation, using the volumetric rate of entropy generation, can be computed by using the resulting velocity and temperature fields. This would involve the skills of numerical thermoflow. The volumetric entropy generation rate formula may be used to derive irreversibility profiles or maps for convective heat transfer arrangements in which the temperature and velocity gradients are known at each point in the medium (Yilmaz et al., 2001).

Hesselgreaves (2000) performed optimisation of heat exchanger surfaces using local entropy generation. Lerou et al. (2005) did heat exchanger optimisation based on a model which divided the counterflow heat exchanger into a number of elements, each sub-divided into three sub-elements: high-pressure gas-element, material element and low-pressure gas-element. For each sub-element, a heat balance equation for the different heat flows was formulated.

2.6.4.2.5 Heat exchangers

Thermodynamic optimisation can be used for many different heat exchangers in different applications. The irreversibility in a heat exchanger is the sum of the associated irreversibilities of each of the two surfaces of the heat exchanger (Bejan, 1982; Bejan et al., 1996). Work was done

on second law aspects of heat exchanger performance (Bejan, 1982) and ways of reducing irreversibility production were proposed. Two factors, temperature difference and frictional pressure drop, are to blame for irreversibilities in heat exchangers (Bejan, 1982; Oğulata et al., 2000; Yilmaz et al., 2001). Yilmaz et al. (2001) imply that the greatest source of dissipative action comes from fluid friction in the form of pressure drop and they also group evaluation techniques for heat exchangers into two classes: techniques using entropy and techniques using exergy as evaluation parameter. Yilmaz et al (2001) emphasise a second law analysis. Bejan (1982) suggests that an efficient heat exchanger has to be large, which requires large amounts of exergy for consumption during the manufacturing process, exergy loss or capital invested in the hardware. He suggests that a comprehensive optimisation programme, which includes this capital, should be undertaken in the field, in cases of specific units for specific jobs. The exergetic efficiency for a heat exchanger (Figure 2.28) with hot stream (1 - 2) and cold stream (3 - 4) is given by equation 2.15 (Bejan et al., 1996):

$$\varepsilon = \frac{\dot{E}_3 - \dot{E}_4}{\dot{E}_1 - \dot{E}_2} \tag{2.15}$$

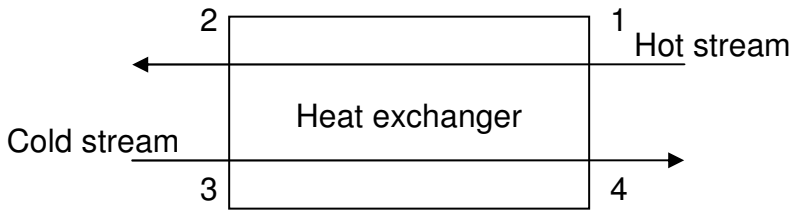

Figure 2.28 Heat exchanger with hot stream (1 – 2) and cold stream (3 – 4).

Sarangi and Chowdhury (1982) expressed the entropy generation in a counterflow heat exchanger and a nearly ideal heat exchanger. The contribution of fluid friction to the entropy generation was neglected. Adiabatic ends were also assumed for the heat exchanger with no heat loss to the surroundings.

Exergetic optimisation was done for tubular heat exchangers. Cornelissen and Hirs (1997) did an exergetic optimisation of a heat exchanger by taking into account the irreversibilities due to frictional pressure drop, the temperature difference between the hot and cold stream and also the irreversibilities due to the production of the materials and the construction of the heat exchanger. Cornelissen and Hirs (1997) mention the LCA method (life cycle analysis), which includes the exergetic effects of all the phases of production, use and recycling, on the environment. A balanced water-to-water counterflow heat exchanger was optimised, neglecting heat loss to the

environment from the heat exchanger and heat resistance of the tube walls. Zimparov (2001) included the effect of fluid temperature variation along the length of a tubular heat exchanger.

Second law analysis and optimisation were done for heat exchangers with ideal gas flow. Hesselgreaves (2000) considered heat exchangers with zero and finite pressure drop. When looking at zero pressure drop, Hesselgreaves (2000) included balanced counterflow, flow imbalance, unbalanced counterflow, parallel flow, condensing on one side and evaporation on one side. The optima for these cases were given. Hesselgreaves (2000) found that, for zero pressure drop, flow imbalance increases entropy generation. Also, it is advantageous to let the highest capacity rate stream be the hot stream. Hesselgreaves (2000) suggests that counterflow should be used, rather than parallel flow, if the heat capacity ratio is small.

Oğulata et al. (2000) did an analysis for a cross-flow plate-type heat exchanger with unmixed fluids and balanced cross-flow. A recuperative plate-type heat exchanger generally used in air or gas applications was examined. Thermodynamic analyses for the balanced cross-flow recuperative plate-type heat exchanger with unmixed fluids were done by Oğulata et al. (2000). Ordóñez and Bejan (2000) did an in-depth numerical optimisation for the parallel-plate heat exchanger with two-fluid ideal gasses, fully developed flow and laminar or turbulent flow. This was done by determining the heat exchanger's architecture using EGM and by constraining the size of the hardware (volume constraint and constraint on the mass of the heat exchanger). All of the lengths which defined the geometry of the heat exchanger were non-dimensionalised.

Ordóñez and Bejan (2000) also included the effect of discharge on entropy generation in a separate analysis of the heat exchanger. Hesselgreaves (2000), Oğulata et al. (2000) and Ordóñez and Bejan (2000) suggest that the $\varepsilon - NTU$ (effectiveness – number of transfer units) method, based on the second law of thermodynamics, can be used to get the outlet temperatures and the total heat transfer from the hot fluid to the cold fluid.

EGM has been utilised in various other applications. Shiba and Bejan (2001) optimised a counterflow heat exchanger that served as a condenser in a vapour-compression-cycle refrigeration system for environmental control of aircrafts with three degrees of freedom and which was subject to two global constraints. It was shown that the minimisation of the total power requirement was completely equivalent to the minimisation of entropy generation rate in the entire installation.

Ishikawa and Hobson (1996) established a thermodynamic optimum surface area for a heat exchanger in an acoustic standing wave (thermoacoustic engine) by minimising entropy

generation due to fluid flow and heat transfer losses. Lerou et al. (2005) optimised a counterflow heat exchanger geometry through minimisation of entropy generation for a cooling cycle in cryogenics. They showed that the width, height and length of the flow channels can be optimised by minimising the entropy. In many counterflow heat exchangers, the heat flow through the material in the longitudinal direction is neglected in determining the temperature profile over the heat exchanger. Equation 2.16 (Bahnke and Howard, 1964, cited in Lerou et al., 2005) is a dimensionless parameter that can be used to see if longitudinal conduction can be neglected or not. k is the thermal conductivity of the heat exchanger material and A_c the cross-sectional area. The longitudinal conduction cannot be neglected if λ_{BH} >10^{-2}.

$$\lambda_{BH} = \frac{kA_c}{L\dot{m}c_{p,\min}} \tag{2.16}$$

For heat exchangers used in cryogenics, this parameter might be in the order of 0.01, while for heat exchangers used in solar thermal applications, the parameter is in the order of 10^{-5}, which means that longitudinal conduction through the material can be neglected in determining the temperature profile over the heat exchanger in these systems.

2.6.5 Solar radiation and the second law of thermodynamics

2.6.5.1 Background

Bejan (1982) presents the topic of exergy waste in solar receivers. He mentions three main features that cause thermodynamic irreversibilities in the operation of any solar receiver: heat exchange between the sun and receiver, receiver-ambient heat loss and the internal irreversibility in the receiver (that is upstream, downstream and inside the receiver). Bejan (1982) applied the concept of irreversibility minimisation to a number of simple solar receiver systems: isothermal receivers, non-isothermal receivers (where a stream of single-phase fluid is circulated through the receiver) and time-varying conditions. These relevant equations for the total rate of entropy generation and entropy generation numbers are given in Appendix B.

Narendra et al. (2000) present an exergetic analysis of a solar thermal power system using the Rankine cycle. The energy analysis showed that losses took place at the condenser of the heat engine part, while the exergetic analysis showed that the collector-receiver assembly was the part where the maximum losses occurred.

2.6.5.2 The exergy of sunlight

When deriving the entropy generation rate at the solar receiver, one firstly needs to better understand the exergy of sunlight. Çengel (2006) presents the topics of thermal radiation and radiation heat transfer from a heat transfer view. According to Çengel (2006), the electromagnetic radiation emitted by the sun is known as solar radiation and nearly all of it falls in the wavelength band of 0.3 – 3 μm. Almost half of the solar radiation is light (visible) and the remaining part is ultraviolet and infrared.

The exact exergy of solar radiation depends on direct and diluted radiation components, the time of day, season of the year, geographic location, and local weather and landscape. It could be determined with spectral measurement and calculation according to Petela (2010). The concept of solar exergy maps was also developed (Joshi et al., 2009).

The solar exergy field was covered extensively by Bejan (1982), who regarded the mission of harvesting solar energy as the placing of exergy at the disposal of humanity for consumption. The sun is regarded as an exergy-rich source and qualifies as a high-temperature fuel. Bejan (1997) presents the thermodynamic properties of thermal radiation in detail. A shift from the heat transfer view of thermal radiation to the thermodynamic view is presented. Bejan (1982; 1997) presents the entropy and exergy (emitted per unit area and per unit time) of blackbody radiation respectively. The entropy of blackbody radiation was found to be a function of temperature only. A collection and interrelation of the fundamental concepts about the second law analysis of thermal radiation are available (Agudelo et al., 2010).

Bejan (1997) gave the entropy generation involved with the transformation of solar radiation into mechanical power (see Appendix B). These include adiabatic free expansion, the transformation of monochromatic radiation into blackbody radiation, scattering and net radiative heat transfer. In the Brayton cycle, adiabatic free expansion and net radiative heat transfer can be excluded. When considering the Gouy-Stodola theorem extended to solar collectors, as described in the literature, Bejan (1982), states that "*the task of maximising the exergy delivered by a collector of fixed cross-section* A_c*, is equivalent to minimising the rate of entropy generation in the 'column' of cross-section* A_c*, extending from the environment temperature* T_0*, to the apparent sun temperature as an exergy source* T^**."* Thus, when the maximum exergy that can be delivered by a collector is considered, the minimisation of the entropy generation rate involved with the transformation of monochromatic radiation into blackbody radiation and the minimisation of the entropy generation rate involved with scattering should be included.

The entropy generation rate due to the transformation of monochromatic/spectral radiation into blackbody radiation, which typically happens at a receiver that is modelled as a blackbody, will be considered first.

2.6.5.2.1 The entropy generation rate involved with the transformation of monochromatic radiation into blackbody radiation

Figure 2.29 gives the entropy increase associated with the constant-energy transformation of monochromatic radiation into blackbody radiation as a function of a dimensionless frequency: $h\nu / kT$. It can be shown that

$$h\nu / kT = 1.439 / \lambda T , \tag{2.17}$$

since it is given that $h\nu / kT$ = 3.921 (the minimum) can be written in terms of the wavelength as: $\lambda T = 0.367$ cmK. This minimum is close to the maximum of the spectral energy distribution located at λT = 0.29 cmK (Çengel, 2006). Thus, for solar radiation falling in the wavelength band of 0.3 – 3 μm, this is equivalent to $0.168 < \lambda T < 1.68$ cmK, where the lowest entropy generation rate is located at λT = 0.367 cmK. This range is also equivalent to: $0.8565 < h\nu / kT < 8.565$. From Figure 2.29, follows that, for this solar radiation range, the entropy increase associated with the transformation of monochromatic radiation into blackbody radiation is close to the minimum.

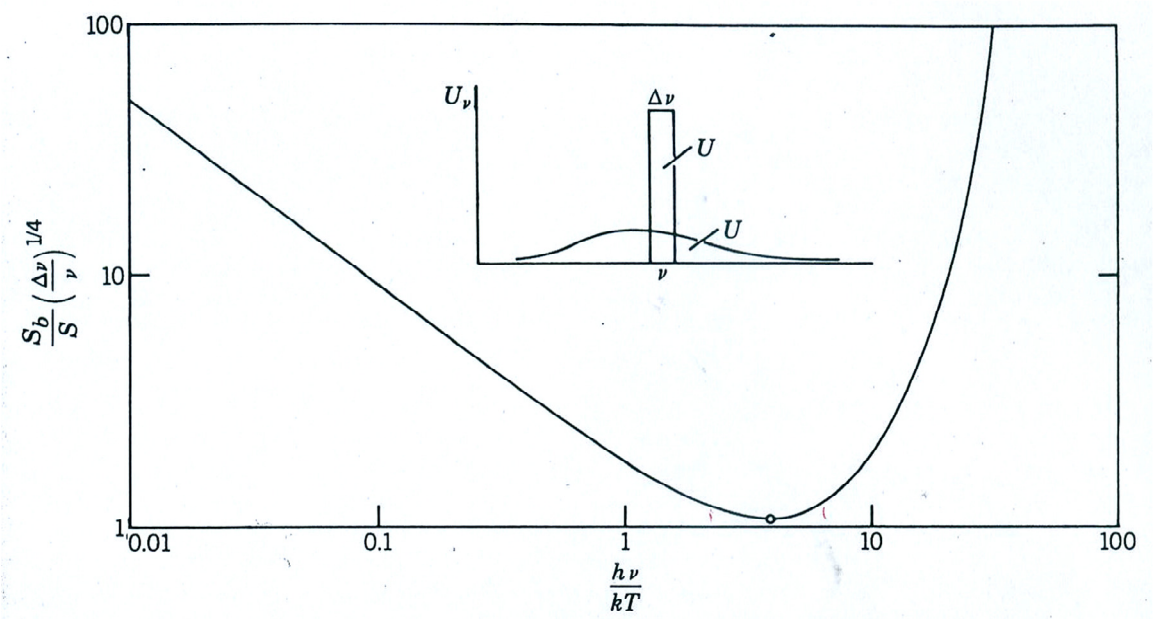

Figure 2.29 The entropy increase associated with the constant-energy transformation of monochromatic radiation into blackbody radiation (Bejan, 1997).

2.6.5.2.2 The entropy generation rate involved with scattering

"In a concentrating device, the maximum theoretical temperature that might be realized at the focal point of a parabolic mirror is that of the radiation beam itself" according to Bejan (1997). When a mirror is assumed to be a specular reflector, this maximum temperature would be the temperature of the sun. One would like to understand the effect of a diffusely reflecting surface on the beam temperature and the entropy generation involved. According to Bejan (1997), scattering from a concentrator decreases the temperature of the original radiation. The decrease in temperature is shown in Figure 2.30 as a function of the dimensionless frequency, hv/kT. From Section 2.6.5.2.1, it is clear that solar radiation falls in the range of $0.8565 < hv/kT < 8.565$. Hence, the temperature ratio from Figure 2.30 will be in the range of 0.07 < T_2 / T_1 < 0.7 due to scattering. With reference to the detail in the top left of Figure 2.30, a solar radiation beam is scattered over a solid angle, $\Omega_2 = 2\pi$ (diffuse reflection by an opaque non-absorbing surface), which is greater than the original angle, Ω_1. T_1 and T_2 represent the monochromatic radiation temperatures before and after scattering.

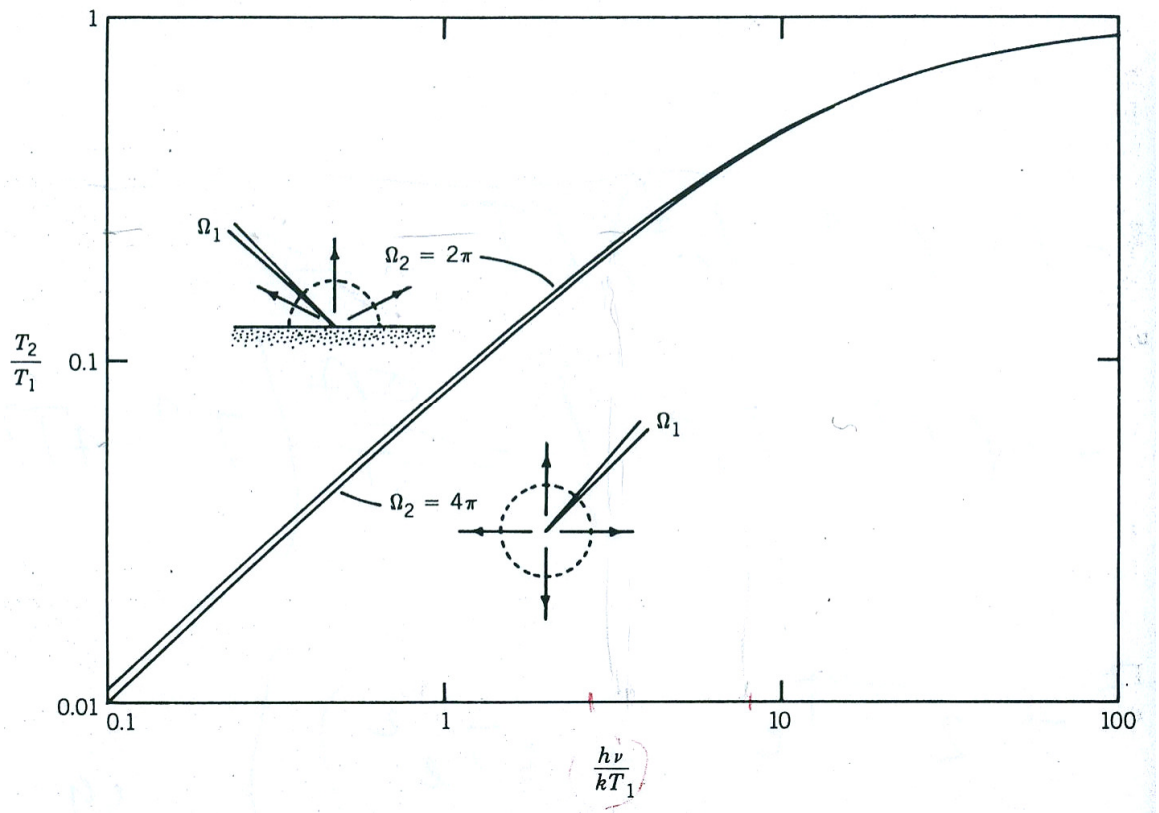

Figure 2.30 The temperature decrease induced by scattering as a function of the dimensionless frequency (Bejan, 1997).

This means that if the sun's temperature is 5 600 K, the monochromatic radiation temperature after scattering would be 393 K – 3 930 K. This temperature decrease causes entropy generation as depicted from the equation given in the entropy generation table (Appendix B, equation 26).

Bejan (1982) gave the exergy of sunlight as:

$$E^* = Q^* \left(1 - \frac{T_0}{T^*} \right) \tag{2.18}$$

where T^* is the equivalent temperature of the sun as an exergy source.

The selection of the control volume around the solar thermal Brayton cycle is very important. If the concentrator is included in the control volume, it has to be kept in mind that entropy is generated at the concentrator due to scattering. The selection of Q^* for this control volume is also very important. Q^* can be chosen to be the heat available at the cavity receiver after the irreversibilities due to scattering and the transformation of monochromatic into blackbody radiation has been deducted.

In this work, the aim is not to determine the precise amount of power available for utilisation at the receiver - methods for determining the exact exergy of solar radiation are available (Petela, 2010; Joshi et al., 2009; Agudelo et al., 2010). The aim is to determine the optimum utilisation of the typical available power at the receiver, with an optimum design.

The available power from the sun varies throughout days, months and environmental conditions. For a steady-state analysis, the power available from the sun is a constant. When assuming a concentrator efficiency, and using a receiver-sizing algorithm (Appendix A) to determine the total intercepted power and heat loss rate at the cavity aperture, the amount of power available for the working fluid in the receiver can be calculated. The aim would then be to determine the optimum utilisation of this available power at the receiver, with an optimum design.

For a control volume around the solar thermal Brayton cycle, the concentrator can be excluded and it can be assumed that T^* = 2 470 K (which is in the range of 393 K – 3 930 K), half of the sun's temperature, since the equivalent temperature of the sun as an exergy source is only 7 - 70% of the sun's temperature after scattering. Bejan (1982) also mentions that Bosjnakovic showed in 1979 that the absolute temperature achievable in a collector is about half of the sun's temperature due to optic limitations.

For the analysis in this work, T^* will be assumed to be 2 470 K at a point between the concentrator and receiver. By doing this, the solar concentrator is not regarded as an entropy-generating mechanism in the analysis. Also, Q^* crossing the boundary of the control volume is the intercepted heat flux at the cavity receiver after the irreversibilities due to scattering and the transformation of monochromatic into blackbody radiation have been deducted.

2.6.6 Exergy analysis for a system as a whole

Narendra et al. (2000) did an exergetic analysis of a solar thermal Rankine heat engine. This analysis was done for the whole system to show the irreversibilities at each part in the system. The collector-receiver assembly was found to be the part where the losses were a maximum. Jubeh (2005) did an exergy analysis for a regenerative Brayton cycle with isothermal heat addition and an isentropic compressor and turbine.

2.6.7 Entropy generation rate equations useful in solar thermal power cycles

Table 2.4 gives a summary of the different entropy generation research fields discussed up to now. This might be a useful starting point for solar thermal power research, where a system with many individual components should be optimised as a whole. This table is useful for identifying entropy generation mechanisms in the solar thermal Brayton cycle. The entropy generation equations from each of these research fields are summarised in the entropy generation table (Appendix B).

The entropy generation rate per unit tube length of circular tube (equation 3, Appendix B) with single-phase fluid and constant heat flux is shown as an example in equation 2.19 (Bejan, 1996). In this equation, D is the tube diameter. This equation shows how thermodynamics is combined with heat transfer and fluid mechanics. An optimum tube diameter, for fixed mass flow rate and heat transfer rate, can be obtained with this equation. When this optimum is available, the entropy generation number can be derived, showing the performance of any design relative to the optimal design. In the literature there are many different ways of non-dimensionalising the entropy generation equations and, therefore, the entropy generation equations are given in Appendix B and not the entropy generation numbers. Appendix B shows all the entropy generation rate equations mentioned in the preceding sections.

$$\dot{S}'_{gen} = \frac{\dot{Q}'^2}{\pi k T^2 Nu} + \frac{32\dot{m}^3 f}{\pi^2 \rho^2 T D^5} \tag{2.19}$$

Table 2.4 A summary of entropy generation literature.

	Entropy generation research field		References
1	**Internal flow**	Internal duct flow (for constant heat flux)	Bejan (1982); Bejan et al. (1996); Hesselgraeves (2000); Yilmaz et al. (2001); Zimparov (2001); Ratts and Raut (2004); Zimparov et al. (2006c)
		Internal duct flow (for constant wall temperature)	Zimparov et al. (2006a)
		Internal duct flow for circular tube (for constant heat flux)	Bejan (1982; 1996); Bejan et al. (1996); Hesselgreaves (2000); Zimparov (2001)
		Internal duct flow for circular tube (for constant wall temperature)	Yilmaz et al. (2001)
		Internal duct flow channel in heat exchanger	Bejan (1982); Bejan et al. (1996); Lerou et al. (2005)
2	**External flow**	External flow	Bejan (1982; 1996); Bejan et al. (1996)
3	**Fins**	For a single fin	Bejan (1982); Bejan et al. (1996)
4	**Local entropy generation**	Local rate of entropy generation (volumetric / 2D)	Bejan (1982); Bejan et al. (1996); Yilmaz et al. (2001); Hesselgreaves (2000)
5	**Heat exchangers**	Counterflow heat exchanger with zero pressure drop	Bejan (1982); Hesselgreaves (2000)
		Counterflow heat exchanger (balanced / unbalanced flow / constant heat flux / ideal gas, etc.)	Bejan (1982; 1997); Sarangi and Chowdhury (1982); Bejan et al. (1996); Cornelissen and Hirs (1997); Ordóñez and Bejan (2000); Yilmaz et al. (2001); Hesselgreaves (2000); Lerou et al. (2005); Zimparov (2001); Ordóñez and Bejan (2000)
		Cross-flow plate-type heat exchanger	Oğulata et al. (2000)
6	**Solar receiver**	Solar receiver (exergy of sunlight, transformation of monochromatic radiation into blackbody radiation, scattering)	Bejan (1982; 1997); Narendra et al. (2000)
7	**Whole system**	Exergy analysis for a solar thermal Rankine heat engine	Narendra et al. (2000)
		Exergy analysis of a regenerative Brayton cycle	Jubeh (2005)

2.7 Useful information, guidelines and points to ponder

- Useful design guidelines, according to Bejan et al. (1996):
  - Keep it simple
  - Consider standard equipment
  - Avoid processes requiring excessively large or small thermodynamic driving forces (differences in temperature, pressure)
  - Maximise the use of co-generation of power
  - Use efficient compressors and turbines
  - Avoid heat transfer at high temperatures directly to the ambient

- Bejan et al. (1996) gave guidelines for evaluating and improving thermodynamic effectiveness:
  - Maximise the use of cogeneration when feasible
  - Minimise the use of combustion
  - Centre efforts on exergy destruction that can actually be avoided
  - Pay more attention to the design of the lower temperature stages of turbines and compressors
  - The lower the temperature level, the greater the need to minimise friction

- Sama (1995) gave very useful guidelines for optimisation using second law insight. Summarised and of most relevance are:
  - Do not use excessively large or small thermodynamic driving forces
  - Do not discard heat at high temperatures to the ambient or to cooling water
  - Try to match heat exchange streams so that final temperature of one is close to initial temperature of the other
  - Choose similar flow heat capacities for the heat-exchanging streams
  - Minimise the use of intermediate heat transfer fluids when exchanging heat between two streams
  - Do not concentrate on the second law inefficiencies which cannot be avoided

- In thermal design and optimisation, two types of independent variables are identified: decision variables (varied in optimisation studies) and parameters (remain fixed). All other variables are dependent variables (Bejan et al., 1996).

- Three problems are encountered in the engineering of solar energy utilisation: low flux density (large surfaces necessary), most solar energy falling on remote areas (transport would be required) and intermittency (little or no power available during bad weather and at night creates a storage need) (Kreith and Kreider, 1978).

- The importance of complying with governmental and environmental regulations throughout the design process as well as the importance of safety, reliability, maintainability and availability (Occupational Safety and Health Acts, published codes and standards, and the Thomas Register) is emphasised by Bejan et al. (1996).

- Shiba and Bejan (2001) argue that the thermodynamic optimisation of the entire system can be pursued on two routes: by either minimising the total power requirement (in the refrigeration case) or by minimising the total rate of entropy generation.

- The internal geometric configuration of a component can be derived by optimising the global performance of the installation that uses the component (Shiba and Bejan, 2001). It is suggested that thermodynamic optimisation by itself (without cost minimisation) may be used in the preliminary stages of design to identify trends and the existence of optimisation opportunities. In the end, the most realistic model is optimised from the start based on cost optimisation. This is also suggested by Ordóñez and Bejan (2000), who furthermore suggest that an entire system can be conceived from the beginning as a system designed to perform certain global objectives optimally, not as an ensemble of already existing parts. According to Bejan et al. (1996), "when a system consists of several components, the overall system should be optimised, since the optimisation of components individually, usually does not guarantee an optimum for the overall system."

2.8 Comments and literature review

The open and direct solar thermal Brayton cycle with counterflow plate-type recuperator, modified cavity receiver and micro-turbines from Garrett will be used in the analysis. A maximum receiver temperature will be specified due to material constraints. A parabolic dish concentrator with 45° rim angle, two-axis tracking and concentrator reflectance larger than 90% will be used.

The second law of thermodynamics and its application in various research fields were shown. EGM was applied in various applications. From the literature, the following general observations and statements can be made:

- Many EGM studies have been done for individual components, but little work has been done on total EGM of overall systems,
- Bejan et al. (1996), Shiba and Bejan (2001) and Ordóñez and Bejan (2000) emphasise that when a system consists of several components, the overall system should be optimised, instead of the optimisation of components individually.

Throughout the literature it is suggested that the overall system should be optimised, since the optimisation of components individually usually does not guarantee an optimum for the overall system. Therefore, the analysis will be done by looking at the solar thermal power system as a whole. Entropy-generating mechanisms can now be identified in the solar thermal Brayton cycle and the total entropy generation can be minimised by optimising the geometry of the components. The apparent temperature of the sun as an exergy source will be assumed to be 2 470 K and at a position between the concentrator and the receiver. An average irradiance of 1 000 W/m^2 will be assumed.